AD A119342

FRANK J. SEILER RESEARCH LABORATORY

FJSRL-TR-82-0007   AUGUST 1982

AN INVESTIGATION OF THE DYNAMIC RESPONSE
OF A SEISMICALLY STABLE PLATFORM

FINAL REPORT

DTIC
SEP 1 7 1982

MR. BILL J. SIMMONS
MAJOR FRANCIS S. HEMING, JR.
MAJOR FELIX E. MORGAN

APPROVED FOR PUBLIC RELEASE;
DISTRIBUTION UNLIMITED.

PROJECT 2304-F2-66

AIR FORCE SYSTEMS COMMAND

UNITED STATES AIR FORCE

82 09 17 039

This document was prepared by the Guidance and Control Division, Directorate of Aerospace-Mechanics Sciences, Frank J. Seiler Research Laboratory, United States Air Force Academy, Colorado. The research was conducted under Project Work Number 2304-F2-66, An Investigation of the Dynamic Response of a Seismically Stable Platform. The project was a joint FJSRL/USAFA faculty effort. Mr. Bill J. Simmons (FJSRL) was the Project Engineer in charge of the work and performed experimental tasks, Major Francis S. Heming, Jr., (DFEM) was Principal Investigator and performed NASTRAN analyses tasks, and Major Felix E. Morgan (DFACS) performed controls analyses.

When U.S. Government drawings, specifications or other data are used for any purpose other than a definitely related Government procurement operation, the Government thereby incurs no responsibility nor any obligation whatsoever, and the fact that the Government may have formulated, furnished or in any way supplied the said drawings, specifications, or other data is not to be regarded by implication or otherwise, as in any manner licensing the holder or any other person or corporation or conveying any rights or permission to manufacture, use or sell any patented invention that may in any way be related thereto.

Inquiries concerning the technical content of this document should be addressed to the Frank J. Seiler Research Laboratory (AFSC), FJSRL/NH, USAF Academy, Colorado 80840. Phone AC 303-472-3502.

This report has been reviewed by the Commander and is releaseable to the National Technical Information Service (NTIS). At NTIS it will be available to the general public, including foreign nations.

This technical report has been reviewed and is approved for publication.

BILL J. SIMMONS
Project Engineer

THEODORE T. SAITO, Lt Col, USAF
Director
Aerospace-Mechanics Sciences

WILLIAM D. SIURU, JR., Colonel, USAF
Commander

Copies of this report should not be returned unless return is required by security considerations, contractual obligations, or notice on a specific document.

Printed in the United States of America. Qualified requestors may obtain additional copies from the Defense Documentation Center. All others should apply to: National Technical Information Service
5285 Port Royal Road
Springfield, Virginia 22161

REPORT DOCUMENTATION PAGE		READ INSTRUCTIONS BEFORE COMPLETING FORM
1. REPORT NUMBER FJSRL-TR-82-0007	2. GOVT ACCESSION NO. AD-A119342	3. RECIPIENT'S CATALOG NUMBER
4. TITLE (and Subtitle) An Investigation of the Dynamic Response of a Seismically Stable Platform		5. TYPE OF REPORT & PERIOD COVERED FINAL REPORT March 1980 - Sep 1981
		6. PERFORMING ORG. REPORT NUMBER
7. AUTHOR(s) Mr. Bill J. Simmons Major Francis S. Heming, Jr. Major Felix E. Morgan		8. CONTRACT OR GRANT NUMBER(s)
9. PERFORMING ORGANIZATION NAME AND ADDRESS FJSRL/NHL (AFSC) USAF Academy Colorado Springs, Colorado 80840		10. PROGRAM ELEMENT, PROJECT, TASK AREA & WORK UNIT NUMBERS DRS 61102F 2304-F2-66
11. CONTROLLING OFFICE NAME AND ADDRESS FJSRL/NHL (AFSC) USAF Academy Colorado Springs, Colorado 80840		12. REPORT DATE August 1982
		13. NUMBER OF PAGES 77
14. MONITORING AGENCY NAME & ADDRESS(if different from Controlling Office)		15. SECURITY CLASS. (of this report) UNCLASSIFIED
		15a. DECLASSIFICATION/DOWNGRADING SCHEDULE

16. DISTRIBUTION STATEMENT (of this Report)

Approved for Public Release: Distribution Unlimited.

17. DISTRIBUTION STATEMENT (of the abstract entered in Block 20, if different from Report)

18. SUPPLEMENTARY NOTES

19. KEY WORDS (Continue on reverse side if necessary and identify by block number)

Gyro Tests
Inertial Sensors
Motion Control
Vibration
Geokinetics

Structural Dynamics
Structural Analysis
Modal Analysis
Finite Element Analysis

20. ABSTRACT (Continue on reverse side if necessary and identify by block number)

A sub-seismically quiet test platform is currently in development at Holloman AFB, NM. Support to this effort includes structural analyses toward design of a platform which has no structural resonances which affect the active servo frequency band. This report describes the analyses performed to establish credibility of methodology by comparison of experimental test analysis and theoretical analysis of structures. Following technique verification, an experimental analysis of Holloman's prototype platform was conducted and results compared to a theoretical analysis. Included in the

DD FORM 1473 EDITION OF 1 NOV 65 IS OBSOLETE
1 JAN 73

Block 20 Continued:

report are descriptions of design requirements, experimental equipment and
techniques, the experimental structural analysis program, the system analysis
for active control, and a comparison of test results to theoretical analyses
results.

Accession For

NTIS	
DTIC	
U	
J	

By
Distr

Avail

Dist

A

TABLE OF CONTENTS

TABLE OF CONTENTS CONTINUED

LIST OF FIGURES

LIST OF FIGURES CONTINUED

1. INTRODUCTION

The prototype active control, isolation test platform currently in development at Holloman AFB, NM, is a major milestone in a program aimed at providing an inertial instrument test facility with motion stability of the order of 10^{-9}g from DC to 100 Hz. The need for such a stable test base was recognized early in the program initiated to develop the more accurate "third generation" inertial instruments, the TGG, Third Generation Gyro, and SFIR, Specific Force Integrating Receiver, accelerometer.[1,2] Plans for development of a precision guidance test facility were disclosed in 1979.[3] The USAF development at the AF Academy of an active control isolation test pad, the ISO-PAD, by the Frank J. Seiler Research Laboratory, provided a basis for determining problems associated with a 6-degree of freedom, active control test platform and the feasibility of eventual compliance with the stability objectives. The ISO-PAD achieved about 10^{-8}g stability over most of the frequency band of interest.[4] A major problem limiting further stability improvement in the ISO-PAD is the location of several modes of structural resonance at low frequencies; these resonant modes limit the active control gain. This problem was considered and a lower limit placed on the structural resonance frequencies in the design requirements of Holloman AFB's prototype seismically stable platform (SSP).

The design analysis of the SSP, using the STARDYNE finite element analysis program, has been covered by the contractor, the Measurement Analysis Corporation.[5] As a parallel effort, experimental and theoretical analyses tasks were performed at the Air Force Academy in support of the Holloman AFB (HAFB) project. Both experimental analysis by a computer analysis program and a theoretical analysis were performed on several structures, and results compared. Following verification of experimental and theoretical techniques, an experimental analysis by MODAL-PLUS of HAFB's prototype SSP was conducted and compared to the contractors theoretical analysis. These efforts and the results were described in a 1981 AIAA paper.[6]

A further task under the Work Unit was an analysis of the active controls of Holloman AFB's SSP. A theoretical analysis of the proposed controls concept for the two-stage system was performed. Experimental

response data was taken of the passive (non-controlled) SSP, and used to refine the theoretical controls analysis. These results were briefed to the HAFB bidders conference for the next development phase, and are documented in this report.

2. BACKGROUND

As a brief explanation of the problem caused by structural resonance on the limits of motion stability which can he otained by the active control, consider the following information derived from the ISO-PAD final report.[4]

First, by way of some understanding of the structure, the ISO-PAD is illustrated in Figure 1. Pertinent to the structural resonance problems are the physical construction of the platform, and the nature of the active controls. The pneumatically supported structure is 25 x 25 x 9 ft and weighs 430,000 lbs. Twenty pneumatic isolators supply the lift force to support the steel reinforced concrete ISO-PAD. The controls on the system are of two types. A low frequency tilt control, with a 10^{-9} arc second sensitivity, 2-axis tiltmeter as sensor, provides correction signals by changes in air pressure on the four pair of outside pneumatic isolators. The air pressure in the 12 inside isolators is controlled to maintain a null position of a sensitive height sensor. The 6-degree-of-freedom high frequency controls are based on seismometers as sensors. Linear and angular velocities are derived from four vertical and four horizontal seismometers. Counter forces to correct for platform motion in the frequency band 0.1 to 20 Hz are applied to eight electromagnetic shakers. This system has been described in some detail in several papers.[4,7] An open loop transfer function bode plot of one servo loop, Figure 2, indicates the problem of obtaining greater motion stability by means of increasing gains. The high gain peaks at 65, 125, etc., are results of structural resonances. The two pole pneumatic isolator/ISO-PAD natural frequency of 1.3 Hz (Horizontal axis rotation) results in the desired roll-off in transmissibility but with the attendant 180° phase shift. Other system elements such as the instruments, shakers, concrete structural damping, and mounting brackets, add to the total phase shift with the result that within the band of interest, the phase margin is

2

poor. The effects of structural resonance near the control band adds to this problem and limits the gain which can be applied. Lead compensation and a 65 Hz notch filter were used, but to a limited advantage due to such poor initial phase margin.

3. OBJECTIVES

3.1 Stability Problem

The SSP active control problem is compounded beyond the structural resonances effects in two important ways. First the long range goals for motion stability are about an order-of-magnitude improvement, to 10^{-9}g; this in itself is an increase in the difficulty of finding a controls system solution. And, this desired stability improvement was a key factor in the inclusion in the SSP design concept of a two-stage pneumatic isolation system for an increase in rate of attenuation with an increase in frequency above the natural spring/mass frequencies of the pneumatic isolation system. The two-stage design approach, essentially two pneumatic spring/mass systems, is shown in Figures 3 and 4. This system is a new approach to motion isolation of inertial test platforms, and no known active control system development has been performed on a similar system.

3.2 Structural Problem

The design objective for minimum structural resonance frequency of the seismically stable platform, SSP, structure was initially established as 200 Hz, an octave above the maximum frequency of interest. The contractor's conceptual design approach included a dual-isolator and two mass structures (Figures 3 and 4). This concept provides a faster, 4-pole, roll-off in motion transmissibility from the pneumatic spring/ mass natural frequency. This additional attenuation would alleviate the resonance problem and the 200 Hz minimum frequency was relaxed to 156 Hz for the primary structure. The intermediate structure was designed to have a minimum resonance of 118 Hz.

3.3 Approach To Problem

The future, ideal SSP, and the related "quiet lab" facility items with closely controlled interface features, will be an expensive fabrication project. Efforts which would provide a high degree of confidence in theoretical designs and avoid expensive modification is highly desirable. Also, it was desired to obtain dynamic models based on actual performance of existing structures to verify theoretical design parameters and provide actual characteristics as a vital input to controls analyses. The following were identified with the aim of meeting these criteria as principle subtasks for FJSRL/AF Academy support to HAFB:

1. Obtain theoretical dynamic models of existing simple structures by means of a finite element analysis program - NASTRAN.

2. Obtain actual dynamic models of these existing simple structures from experimental test data.

3. Compare Items 1 and 2 results to verify accuracy of the two techniques.

4. Obtain both experimental and theoretical analyses of a complex structure (the ISO-PAD).

5. Compare results of Item 4 to verify the techniques as applied to complex structure models.

6. Obtain the actual dynamic model of the prototype SSP structure for comparison to the contractor's design requirements and theoretical analysis by STARDYNE. An important task is that the experimental model be made available as an input to the development of the SSP active control system.

7. Perform a controls analysis of the two-stage system, refined with real data from the fabricated passive SSP.

These support tasks to Holloman AFB complement a more general task of establishing the capability to perform instructional problems and demonstrations in the dynamics analysis course work at the AF Academy. This effort also supports effort which was part of the original objectives, but dropped pending completion of the SSP, namely an advanced system design by NASTRAN, and test of a scale model representative of the advanced-SSP system design.

4

4. THEORETICAL STRUCTURAL ANALYSIS TECHNIQUES

Finite element analyses were made of the simple structures (a cantilever beam and a fixed plate) and of the ISO-PAD. The data obtained was compared with experimental results obtained from the actual structures. The purpose of these analyses and comparisons was to verify the finite element models so that they could be used as design tools to determine the effect of proposed modifcations to the existing structure and to provide the capability for design of an advanced SSP. As the prototype SSP progressed and longer development schedules were protracted, the -66 task of providing a finite element model of the SSP was postponed indefinitely.

Since no large, general purpose finite element program is available on the local computer facility, the ARPANET link was used to gain access to the computer facilities at the Air Force Weapons Laboratory (AFWL), Kirtland AFB, New Mexico. The ARPANET is a network of military and civilian facilities operated by the Defense Communications Agency. The network provides each member a means of access to the computer facilities and software of the other members. The CYBER 750 at AFWL was accessed via the ARPANET to perform MSC/NASTRAN (MacNeal-Schwendler/NASA STRUCTURAL ANALYSIS PROGRAM) analyses of the structures mentioned.

5. EXPERIMENTAL PROVISION

5.1 General

Selections of additional test equipment and software were made with consideration of the test specimens' characteristics, the frequency band of interest, and existing equipment which could be committed to the project. It was desired that all additions be general purpose to the extent that would provide adequate performance for the planned tests of the SSP, ISO-PAD, and simple structures. The equipment obtained provides adequate signal/noise to measure the important resonances in the frequency band of 10 Hz to 5 KHz.

The Frank J. Seiler Research Laboratory has a PDP 11/05 computer with 32K memory, which had been dedicated to Fourier analysis related to

control problems. The MODAL-PLUS* experimental data analysis program can be operated within this size computer. With some peripheral equipment modification, the MODAL-PLUS program was implemented.

5.2 Experimental Analysis Software (MODAL-PLUS)*

Experimental modal analysis is intended for use where it is required to determine the actual dynamic characteristics of a test structure and obtain a valid and complete mathematical model of the structure. In the early 70's, experimental modal analysis programs were developed for use on minicomputers. This provided easy access to powerful tools for analyzing vibration problems. The MODAL-PLUS Software Package was created by SDRC (Structural Dynamics Research Corporation) for performing experimental modal analysis with a minicomputer. This software package performs a variety of functions, including data collection, analysis, and several display routines. Modal parameters which can be determined are modal mass, modal stiffness, damping, natural frequencies, and mode shapes. An animated display of the structural vibration by mode shape can also be provided. The structure of the MODAL-PLUS software includes five main modal analysis objectives (see Figure 5). Specific functions which are provided include the following:

1. Definition of the structure geometry.

2. Set calibration and conditions for multi-channel acceleration measurements.

3. Calculation of natural frequencies and their associated damping and phase relations.

4. Extraction and display of mode shapes.

The program routines which must be used and a brief description of each are provided in Appendix A.

The MODAL-PLUS program implements both impact and random excitation techniques to be used. Both types of excitation were used in tests of the SSP.

---

*MODAL-PLUS is under copyright by the developer, Structural Dynamics Research Corporation (SDRC).

6

5.3 Test Equipment

The key items required for the experimental tasks of the project are the computer and peripherials used for operation of the MODAL-PLUS software program. This requirement was adequately fulfilled by a PDP 11/45, 32K word computer, with one RK05 auxilliary disk memory, Tektronix 4012 terminal, ACEMUx analog-to-digital signal conditioning equipment by Gen Rad, Inc., and Tektronix 4631 hard copy unit. In order for the program to calculate modal parameters, input data is required in the form of an input reference force signal from a structural exciter and acceleration signals from selected response points. Motion excitation of the structure may be impulse, by use of an impact hammer, or random by use of an electro-mechanical shaker. For the type structures covered here, a PCB K291A impulse hammer kit, LTV 411 shaker, BB&N 507 triaxial accelerometer, and BB&N P-20 charge amplifier were satisfactory. Other equipment required, of normal laboratory quality, were amplifiers, filters, oscilloscopes, and tape recorders. The specific vendors and models of the above equipment are provided only as an indication of the equipment specifications; many equivalent items from other suppliers are available.

6. TECHNIQUE VERIFICATION OF CANTILEVER BEAM

6.1 Test Procedure

The first simple model tested was the cantilever beam. The equipment and MODAL-PLUS set-up for the beam problem is illustrative of the more general structural test. The beam was initally divided into eight 6 inch sections with 9 response point measurements to be taken. In a later analysis, it was divided into sixteen 3-inch sections, in order to increase accuracy and to obtain a smoother curve during animated graphic display of the mode shapes. This test was also performed with both a shaker input and a hammer input. The set-up of the cantilever beam test is shown in Figure 6. The beam selected for a simple structure test is a 6061-T6 aluminum beam, 54 inches long (48" exposed) and 31/32 inches square. The beam is fixed at one end to a heavy steel table; the exposed point of the cantilever beam is identified as Point #1. The 17 points are determined and marked, and acceleration data taken as triggered

7

inputs to the computer resulting from an input of the impulse hammer at the reference point. In this set-up, Point #17 was selected as the reference point for excitation. Time plots of a sample impulse set may be observed on the computer terminal display for purposes of verifying trigger conditions and signal amplitudes. The data for computation of a modal parameter is obtained by striking the beam at the reference point to create motion within the structure, and by collecting acceleration data at all response points. Typically, input data from a point is set-up by the operator to be used as an average of several, say 10, impulse samples. The resultant transfer function bode plot, Figure 7, is used to pick out the resonant frequencies of the beam. The frequencies where the four mode shapes occur are noted on the figure.

The data shown below is a result of impact hammer excitation. Results from random excitation using a shaker were about the same. It is evident from the nature of some structures that an impulse hammer is more conveniently used. The hammer is much more mobile in that it allows the user to strike the structure at any point and in any direction. The shaker, on the other hand, can only shake in one direction and must be securely attached to the structure at one point. One advantage to the shaker, however, is that the motion it creates within the structure is much more uniform. Therefore, the modes are more distinct, easier to read, and possibly more accurate.

6.2 MODAL-PLUS Analysis

The Bode plot of the transfer function result at one response point is shown in Figure 7. Similarly, data from all other response points is obtained, and in MODAL-PLUS, using the PCALC (parameter calculations) and SCALC (shape calculations) routines, the modal coefficients are obtained. The shapes of the first four modes of the cantilever beam are shown in Figures 8 thru 11; these figures are 'stills' of the graphics animated display (ANIMAT Program) on which the phase of the mode is clarified by darkening the extremities of the shape The frequencies of these four modes, shown on the corresonding figure, are identified in Table 1, Beam Mode Verification.

8

6.3 NASTRAN Analysis

The NASTRAN analysis of the cantilever beam was made using the model shown in Figure 12. Eight equally spaced beam elements (CBAR) with two degrees of freedom per node were used resulting in 16 degrees of freedom for the analysis. The natural frequencies and mode shapes for the first four modes were determined using a normal modes analysis (Givens Method). The resulting mode shapes are shown in Figures 13 thru 16. The frequencies along with the exact and MODAL PLUS values are given in Table 1. The comparisons clearly indicate that even though the NASTRAN model is fairly crude, it produces excellent results (as expected for this simple structure).

6.4 Beam Mode Verification

The experimental results using MODAL-PLUS, and the theoretical values obtained using NASTRAN, were compared to theoretical values calculated from ideal beam equations for the first four modes. The equation used for theoretical values was:[7]

$$f_m = \frac{A}{2\pi} \sqrt{\frac{EI}{\mu \ell^4}}$$

where   A is a modal coefficient

       E – Young's Modulus

       I – Area moment of inertia of cross section

       ℓ – length of beam

       μ – mass per unit length

The frequency comparison of MODAL-PLUS, NASTRAN, and an ideal beam calculation of values, is shown in Table 1.

Table 1. Technique Verification, Cantilever Beam

MODE	MODAL-PLUS	NASTRAN	THEORETICAL
F_1	12.95 Hz	13.82 Hz	13.86 Hz
F_2	80.30	85.07	86.89
F_3	222.37	233.94	243.31
F_4	433.88	449.21	476.78

This comparison of modal frequencies is considered good. Small differences of MODAL-PLUS actuals, theoretical NASTRAN, and 'Ideal' values are attributable to several factors including inaccurate location of excitation impact and response points, material characterization, and imperfections in realizing an ideal attachment point.

At this point, we were confident in using and manipulating the 'MODAL-PLUS' software, in the experimental results, and in the NASTRAN analysis technique. It was decided to perform tests on a slightly more complex model for further verification of the techniques of experimental and NASTRAN analyses.

7. TECHNIQUE VERIFICATION OF PLATE

7.1 Test Procedure

For the next step in experimental test complexity, an aluminum plate clamped on all four edges was tested. The test specimen was a 23 3/4 inch square, 3/8 inch thick plate, type 6061-T6 aluminum, which when clamped as shown in Figure 17, has a usable surface of 22 1/4 inch square. The plate was divided into nine active data points by sectioning the plate into 16 segments. Including the stationary points at the edges, a geometry of 25 points is required. Real acceleration data is required at only the 9 active points. The equipment set-up and data collection is essentially the same as that described in the beam tests. The impulse hammer technique was used; point #19 (see Figure 18, the geometry preview) was the reference impact point. Ten samples of acceleration data were averaged as input at each active response point.

7.2 MODAL-PLUS Analysis

The transfer function bode plot generated for response point 19 of the plate is shown in Figure 19. The low frequency resonances are usually quite distinct; however, at higher frequencies the resonances are sometimes hard to determine based only on the response amplitude. Additional information which is helpful in determining which peaks are due to a resonance are the corresponding 180 degree phase shift; also of help are the damping values obtained in parameter calculation (PCALC) and curve fit in shape calculation (SCALC). The resonances are selected from

10

observation of the frequency display plots of all active response points. The larger resonances were at the following frequencies: 230, 491, 704, 785, 942, 1075, and 1391 HZ.

7.3 NASTRAN Analysis

The NASTRAN analysis of the plate was made using the model shown in Figure 20. Sixteen square plate elements (CQUAD) with three degrees of freedom per node (one translation and two rotations) were used. Two models of the plate were analyzed using this grid. The first was a model of the entire plate with all four sides fixed; this resulted in 27 degrees of freedom. The second model used symmetry. A quarter of the plate was analyzed with two sides fixed and with symmetry conditions on the remaining two sides; this resulted in 40 degrees of freedom. The natural frequencies obtained are shown in Table 2 along with the theoretical and MODAL-PLUS results. The first three modes are shown in Figures 21 thru 23 with the arrows indicating the direction and relative magnitude of selected nodal displacements. The mode shapes are identical for the whole and quarter plate models.

7.4 Plate Mode Verification

Calculations were made of theoretical resonant mode frequencies of an 'ideal' plate with the edges fixed.[8] Table 2 shows the comparison of MODAL-PLUS, NASTRAN, and the ideal plate for the first three modes.

Table 2. Technique Verification of Plate

MODE	MODAL-PLUS	NASTRAN (WHOLE)	NASTRAN (SYMMETRY)	THEORETICAL
F_1	230	263	259	244
F_2	491	579	530	502
F_3	704	883	769	697

The MODAL-PLUS errors are probably acceptable when one considers the flexibility of the 'fixed' edges which is allowed by a C-clamp attachment. Fairly good correspondence in results vs ideal plate theory

11

is obtained if the plate is assumed to be 23 3/4 inch square rather than the intended unrestrained 22 1/4 inch. Figure 24 shows the Animation resultant display for these three modes.

The NASTRAN results show the expected convergence toward the theoretical values when more degrees of freedom were added in the symmetry model. Further grid refinement would reduce the 6-10% error to negligible amounts.

The conclusion drawn from the beam and plate simple structures was that test results were a fairly good match with theoretical values. With this background of use of the experimental analysis program on test of simple structures, the equipment set-up was extended to test the complex Iso-Pad and SSP structures. The finite element models also provide excellent results as long as the structure is modeled in sufficient detail.

8. COMPLEX STRUCTURE (ISO-PAD) VERIFICATION

8.1 Iso-Pad Structure

The Iso-Pad (see Figure 1) was briefly described earlier under 'Background'. This large structure of 'cruciform' shape is reinforced concrete. The Iso-Pad structure is now homogenous due to emplacement of weight lightners, termed sono-tubes in one direction, and it is non-symetrically loaded (note the 1500 pound gryo test table is located on the North-Center test pier). The Iso-Pad exhibits relatively large modal damping coefficients but the numerous structural resonances still make further improvement in active control performance impractical. In 1975[7], significant structural resonances were found to exist at 48, 59, 65, 67, 121 Hz and higher frequencies. The Iso-Pad was 'up', that is supported by the 20 pneumatic isolators. The passive system transmissibility rolls off at 40 db/decade, and thus could be considered as a free floating body as far as vibration above 20 Hz was concerned.

8.2 MODAL-PLUS Analysis

MODAL-PLUS was used to determine the natural frequencies and mode shapes of the reinforced concrete Iso-Pad. The structure geometry and

12

node points are shown in Figure 25. Figure 26 provides a modal coordinate listing; note that locations were measured in millimeters. Impact excitation was used at the reference point 32, which is the top SE corner, and the response measured by accelerometer at the modal response points in the z-direction only. The natural frequencies were determined by MODAL-PLUS and are presented in Table 3. (Section 8.4)

The MODAL-PLUS results were compared to the prior, 1975, findings, including modal animation. Again, it should be noted that the 1975 structural resonances were observed in the process of adding six degree-of-freedom active controls to the Iso-Pad. An attempt was made to discover the modes of vibration at that time by rather empirical methods. The MODAL-PLUS results were very illuminating in terms of the mode shapes. For example, the 65 and 67 Hz resonances had been considered, in 1975, to be pure torsion modes, one about an E-W axis, the other about the N-S axis; also, the 121 Hz mode shape was completely undetermined. The actual modal shapes are easily derived from MODAL-PLUS, and are discussed below for the first four modes.

For purposes of simplifying the views of modal animation, the full geometry set of the Iso-Pad is reduced to two geometry traces. The cruciform shape lower section, trace 1, and attached bottom plane of the box section, trace 2, are the solid lines on Figure 27.

'Animation' of the first mode, 46.41 Hz, is shown in Figure 28. The arrows are added to indicate the phase relationship at points of significant motion. Thus, it may be observed that opposite corners of the Iso-Pad are in phase, and the two pair are 180° out of phase. That is, as shown, the NW and SE corners are moving down while the NE and SW corners are moving up.

The second mode, 57.41 Hz, is shown in Figure 29. The motions of all four corners are in phase and this mode could be characterized as the vertical mode.

The 'third' mode, 66.923 Hz, is shown in Figure 30. From the observation that the SE and SW corners are in phase, and 180° out of phase with the other pair, we see that two modes of this type should be identifiable. If we term this mode a torsion mode about the E-W axis, it follows that there should be a torsion mode about the N-S axis at a slightly different frequency due to the non-symmetrical loading. If

13

other impact points were selected for impulse excitation, the N-S 'torsion' mode (65 Hz) should be observed as it is in active servo tests. Another point observed from the MODAL-PLUS extraction was that this 3rd mode is not a true torsion mode; the cruciform section motion complicates that simple description.

The fourth mode, 120.92 Hz is shown in Figure 31. This modal frequency had been identified in 1975; however, the mode shape was not disclosed. It is seen, looking at one edge of trace 2 (the plane), that the fourth mode is a higher order mode of the 1st mode mechanism. Due to the thick cruciform section, there is a non-linear load and stiffness distribution, and the higher mode is not simply a multiple of the 1st mode.

Many other modes were observed with frequencies above the 121 Hz 4th mode and up to the 5 KHz frequency maximum selected in test conditions. These are not shown since only the lower frequency modes are of importance at present.

8.3 NASTRAN Analysis

Two models of the Iso-Pad were used: one of the entire structure and one of a quarter of the structure that uses symmetry about two axes.

The model of the entire Iso-Pad comprised fourteen 20-node solid elements (CHEXA) totaling 136 nodes and 408 degrees of freedom. This model (Figure 32) contains one layer of solid elements in each portion of the Iso-Pad (i.e., the cruciform and the block). A normal modes analysis using the Givens method resulted in the natural frequencies given in Table 3 and the corresponding mode shapes shown in Figures 33 thru 37. The arrows on the mode shapes indicate the direction and relative magnitude of selected nodal displacements.

The symmetry model comprised 28 20-node elements (CHEXA) totaling 232 nodes and 594 degrees of freedom. Two layers of elements were used in both the cruciform and block portions of the Iso-Pad as shown in Figure 38. The inverse power method was used for this analysis resulting in the natural frequencies listed in Table 3. The mode shapes are not shown since they match those obtained with the whole structure model.

14

8.4 ISO-PAD Verification

Table 3 presents frequency data from MODAL-PLUS and NASTRAN analyses and the frequencies determined from the previous experimental investigations in 1975. The MODAL-PLUS results show good agreement with the resonances noted during servo development, and, as noted above in MODAL-PLUS Analysis, clarify the mechanism of the mode shapes.

At first glance, the NASTRAN results are somewhat disappointing since the frequencies are higher than expected. Closer examination shows that the mode shapes (Figures 33 thru 37) match those obtained experimentally, but that the frequencies are 40-50 % high for the whole structure model and 33-40 % high for the symmetry model.

One probable cause of this discrepancy is the material properties used for the NASTRAN analysis. Reinforced concrete can be difficult to model since it is a nonhomogeneous, nonlinear material. For these models, the stiffness (E) was determined from information provided on preconstruction drawings of the Iso-Pad. Although no tests have been performed to determine the actual properties of the concrete used in the structure, it is very likely that they do not match the drawings. Since the natural frequency is roughly proportional to the square root of the stiffness, we can determine the value of E required to produce frequencies comparable to those obtained experimentally. The new value of E is reasonable, but time constraints did not permit additional analyses.

A second cause of the discrepancies is the hollow sono-tubes that run through the structure. The presence of these tubes could have a significant impact on the stiffness properties. It is possible that the tubes decrease the stiffness of the Iso-Pad and result in lower natural frequencies than expected.

Another interesting result of the finite element analyses is the presence of a mode at 81.06 Hz (Figure 34) that was not observed in 1975 with MODAL-PLUS. This mode exhibits out of phase symmetrical bending about both midplanes with nodes occurring at the corners. Since the corner points are nodes, the MODAL-PLUS impulse excitation at one of these corners did not excite this mode.

15

Table 3. Frequency Data from MODAL-PLUS and NASTRAN Analyses

FREQUENCY	OBSERVED 1975	MODAL-PLUS	NASTRAN WHOLE STRUCTURE	NASTRAN SYMMETRY
F_1	48	46.41	64.97	61.64
F_2	--	--	81.06	79.01
F_3	59	57.41	86.08	80.97
F_4	65,67	66.92	95.80	89.73
F_5	121	120.92	167.59	159.16

NOTE: All frequencies are in Hz.

The results generally confirmed prior findings and the validity of MODAL-PLUS and NASTRAN techniques as applied to a complex structure.

9. CONCLUSIONS ON ISO-PAD ANALYSES

The results show that MODAL-PLUS and MSC/NASTRAN provide the analyst with powerful tools for modal analysis. Both approaches can provide a very accurate modal representation of a structure. The MODAL-PLUS results serve to validate the experimental approach used and to demonstrate the usefulness of experimental techniques for analyzing existing structures. The absence of mode two from the results shows that the excitation point should be carefully chosen so that all modes present will appear in the results. The finite element method also provides accurate modal representations, but the results will only be as good as the model and material properties used for input. In addition the finite element model can be used as a design tool to simulate modifications to a structure before resources are committed for the actual fabrication. In these analyses, use of both techniques together allowed validation of the models and would provide high confidence in design results obtained using the finite element model.

16

10. TESTS OF THE SEISMICALLY STABLE PLATFORM (SSP)

10.1 General

At completion of the passive SSP fabrication and installation, it was planned to obtain experimental verification of performance. Particular aspects desired of the performance of the pneumatically isolated, free-floating, or passive, system were verification of contractors structural design, response data for input to an active controls design, as a follow-on development, and verification of the desired 4-pole roll-off attenuation expected from a 2-stage isolation system. The effort on the first two items will be discussed; the results pertaining to the third item were secondary, and since these only verified HAFB tests specifically for the roll-off in attenuation, will not be covered in detail. Suffice to say, attenuation was not as expected, and the explanation may include findings from both the controls analysis and the actual structual resonances of the completed SSP. These three items were key inputs to the SSP status information pertinent to request for bids for a follow-on contract action to develop the instrumentation and active controls system.

10.2 The SSP System

The SSP, Seismically Stable Platform, has been described in detail by the Phase 1 contractor; an AIAA paper by key contractor personnel is one source.[5] For completeness, the SSP system will be described in brief.

The SSP (Figures 3 & 4) is designed to be a very stable test pad on which a gyro test table is mounted; this configuration is to provide motion isolation to sub-seismic levels as a base for next generation, inertial grade instrument evaluation tests. A system concept was proposed, consisting of two stages of spring/mass isolation; this would provide an 80 db/decade roll-off from the natural frequency (F_n). At low frequencies, DC to about 10-30 Hz, where earth and building motion is not sufficiently attenuated, an active control system would sense platform motion and apply corrective torque, thus achieving a motion stability of 0.02 arc sec, 10^{-8}g stability, from DC to 100 Hz. The

17

Phase 1 contract covered conceptual design and fabrication of the 'passive', non-controlled system. Follow-on contracts are planned for development of instrumentation and the active control system.

The SSP system concept includes the existing seismic mass on which the SSP was constructed, the 2-stage pneumatic isolation system, an instrumentation system, and the multi-axis 'active' control system. The overall concept was studied by the Phase 1 contractor, the Measurement Analysis Corporation, and a total system concept proposed. The passive, 2-stage isolation concept was approved, fabricated, and installed in the Advanced Inertial Test Lab (AITL) on an existing seismic mass. The seismic mass is of a design similar to the ISO-PAD base (see Figure 1), namely, a heavy reinforced concrete pad in a crushed granite medium. This design, widely used in other Air Force and industry test facilities, effects moderate attenuation at higher frequencies.

10.3 The SSP Structure

The dual isolation system consists of a primary reaction mass/ structure which supports the instrument test table, a secondary mass/structure required to implement a dual system, 4-pole roll-off in attenuation, and the pneumatic isolation system which supports the two reaction masses. Both structures have two basic requirements, namely, first to provide the physical characteristics to provide a support without low frequency resonances for the inertial instrument test table and the various instruments and actuators which are to be attached for implementation of an active control system. A second basic requirement is that inertial mass be provided to give low values of spring/mass natural frequency of the pneumatic isolation system. Additionally, when the basic form and mass of the primary structure is established, the mass of the secondary structure must be selected to optimize the attenuation characteristics of the dual-isolation system. The final design for the primary structure resulted in a A36 mild steel weldment, about 16 feet across, and estimated to weigh about 16,000 pounds (Figures 3 and 39). The contractors' analysis determined that the secondary structure should be about half the weight of the primary structure; the final design resulted in a weight of about 9,000 pounds (Figures 3 and 40). During design of the structures, the contractor, using the STARDYNE structural

18

analysis program, maintained the requirement of no low frequency reso-
nances. The original goal in minimum structural resonances of 200 Hz was
relaxed during the interim design review to the analysis result values of
155 Hz for the primary structure and 119 Hz for the secondary mass.

10.4 SSP Test Set-up

After fabrication and assembly of the 'passive' SSP at Holloman
several types of performance tests were conducted. The two types of
tests conducted by FJSRL, and for which results are shown, were made on
two occasions. In April 1982, data was obtained pertinent to conducting
the MODAL-PLUS analyses of the structures. The real time data was
recorded for playback and analysis at the Air Force Academy where the
computer and software were available. Previous experience with off-site
recording of data for later analysis indicated significant redundancy is
desirable, and frequent, if not continuous, monitoring of the signals to
avoid recording bad data. The set-up for obtaining structural resonance
data is shown in Figure 41. Using as excitation, first an impulse
hammer, later a random generator excited electromagnetic shaker, the
structures were excited and three axes of acceleration data recorded.
The excitation point (MODAL-PLUS reference point) was fixed for a given
data set, and the three axes of acceleration data was taken from each
response point in a geometry defined in MODAL-PLUS (Figure 42). Two
points not illustrated in Figures 39 and 40 describe the top and bottom
of the instrument test table. Four channels of data, the impact hammer
acceleration and three axes of response acceleration, were continuously
monitored by oscilloscopes. Duplicate tape recordings were made on two
parallel connected recorders, and playbacks of data from each response
observed to ascertain that good data was recorded.

The sets of structural data taken were as follows: impact excitation
data from both structures with reference point 49Z (see Figure 39,
Primary Structure); impact excitation data from the secondary structure
with reference point with mode point 1Z as reference; random excitation
data from the primary structure with mode point 77Z as reference; and
random excitation data from the secondary structure with mode point 107Z
as reference. With the shaker attached at reference point 107 on the

secondary structure, a set of data was taken from both structures for transfer function analysis. All of the vibration test data was taken with the BBN507 accelerometers, PAR #113 amplifiers with 1-pole filters set for a 1-1K Hz pass band, and the random noise generator set for a 10-5 KHz excitation band. This set-up provides best signal/noise in the more important structural resonance band, 20 to 1K Hz, and slightly degraded information on the higher amplitude vibration modes out to 5K Hz.

In August 1981, data was taken with emphasis on the low frequency band of 0.2 - 200 Hz to provide a basis for experimental verification of an active control analysis. Again, data was recorded on tape for analysis at FJSRL. Figure 42 illustrates one of several tests set-up, where the electrical connections, similar to that in Figure 41, have been omitted for clarity. In this set-up, 'true' vertical motion is obtained by adjusting the gain of the South shaker amplifier with respect to the North set to null any angular motion as sensed by a horizontal seismometer. Then the vertical response of the primary structure, as sensed by SL210 vertical seismometers with respect to vertical force is recorded. Other data obtained was simultaneous records of random excitation force and seismometer outputs of both structures for both vertical and angular excitations. It was not practical to input a known motion to the seismic mass and measure the system response, but as will be seen below, a total system response can be implied from the data taken.

10.5 MODAL-PLUS Analysis of Structures

A MODAL-PLUS analysis of the SSP structures was performed for both the impact excitation data and for the random excitation data. The two results should be and are approximately comparible with some differences in modal parameters accountable to excitation techniques and signal/noise variations with frequency. It was expected from SDRC comments on MODAL-PLUS, and S/N levels, that in the band of principle interest, 25-400 Hz, the random excitation technique would be more accurate. Modal parameters determined from the impulse excitation data are shown in Table 4 and parameters resulting from random excitation data are shown in Table 5.

20

Table 4. SSP Modal Parameters by Impulse Excitation

MODE PARAMETERS, PRIMARY MASS

MODE	FREQ (Hz)
1	89.003
2	136.573
3	335.037
4	621.428
5	648.910
6	890.871
7	896.102
8	1456.070

MODE PARAMETERS, SECONDARY MASS

LABEL	FREQ	DAMPING	AMPLITUDE	PHASE	REF	RES	MODE				FLAGS	
1	101.247	0.000551	1.8802E 04	-1.5734	1Z-	1Z+	1	0	0	0	1	1
2	150.089	0.000811	1.0533E 04	-1.5331	1Z-	1Z+	2	0	0	0	1	1
3	279.123	0.006128	3.1902E 04	-1.6901	1Z-	1Z+	3	0	0	0	1	1
4	293.910	0.007010	7.8057E 04	-1.5335	1Z-	1Z+	4	C	0	0	1	1
5	380.258	0.000887	5.9751E 04	-1.6409	1Z-	1Z+	5	0	0	0	1	1
6	431.585	0.010049	2.4720E 04	-1.6149	1Z-	1Z+	6	0	0	0	1	1
7	455.080	0.003754	6.6148E 04	-1.5617	1Z-	1Z+	7	0	0	0	1	1
8	3886.192	0.010154	1.7806E 06	0.3402	1Z-	1X+	8	0	0	0	1	1

Table 5. SSP Modal Parameters from Random Excitation

MODE PARAMETERS, PRIMARY MASS (SSPM3)

MODE	FREQ	DAMPING	AMPLITUDE	PHASE	REF	RES	MODE				FLAGS	
1	40.534	0.034624	1.374	0.1619	77Z+	103Z-	4	0	0	0	1	1
2	60.705	0.073985	2.884	-1.7696	77Z+	106Y+	2	0	0	0	1	1
3	87.029	0.028439	1.151	-1.0411	77Z+	106Y+	1	0	0	0	1	1
4	95.412	0 027452	7.465	1.7920	77Z+	106Z-	3	0	0	0	1	1
5	120.308	0.011578	10.17	-0.3208	77Z+	49Y-	5	0	0	0	1	1
6	142.044	0.003376	22.96	2.7917	77Z+	71Z+	6	0	0	0	1	1
7	253.333	0.008857	117.2	2.5362	77Z+	77Z-	7	0	0	0	1	1
8	294.595	0.007369	340.1	-3.0950	77Z+	77Z-	8	0	0	0	1	1

MODE PARAMETERS, SECONDARY MASS (SSPM2)

MODE	FREQ	DAMPING	AMPLITUDE	PHASE	REF	RES	MODE				FLAGS	
1	22.258	0.097541	5.106	2.3358	107Z+	3X+	1	0	0	0	1	1
2	49.674	0.295532	76.57	1.4840	107Z+	1Z+	2	0	0	0	1	1
3	61.732	0.006579	2.203	1.5322	107Z+	3X+	3	0	0	0	1	1
4	88.136	0.010039	1.294	-1.4319	107Z+	3Z+	6	0	0	0	1	1
5	89.658	0.169813	1215.	2.5139	107Z+	107Z+	7	0	0	0	1	1
6	101.087	0.023537	92.99	-0.4561	107Z+	1Z+	4	0	0	0	1	1
7	278.597	0.008233	115.1	-3.0258	107Z+	1Z+	5	0	0	0	1	1

21

Figures 43 thru 49 show the MODAL-PLUS generated mode shapes, from impulse data, for the lowest natural frequencies when the primary and secondary masses were analyzed as a combined system. Program limitations allow either the primary or secondary mass to be shown individually, but not simultaneously. At the lowest frequency, 89.003 Hz, the primary mass deforms as shown in Figure 43. Again, the arrows are used to indicate the phase relations of the deformations. In this case, the extremities of the primary mass are moving up and down in phase as the "bucket" "swings" from side-to-side. Of all the low frequencies identified, the 89 Hz is the only mode suspect due to very high damping and uncertain phase data; this was later clarified using random excitation data. At 136.573 Hz and 355.037 Hz, Figures 44 and 45, two opposite extremities are moving in one direction while the other two are in opposite phase. In each case, there is distortion at the "bucket" top.

Figures 46 thru 49 show the MODAL-PLUS generated mode shapes for the secondary mass. At the lowest frequency, 101.247 Hz, the structure appears to deform in a simple bending mode as shown in Figure 46. At 150.089 Hz (Figure 47), the complicated deformation pattern can best be described as primarily horizontal movement of the top and bottom surfaces. Also, the rotations which occur about a horizontal axis through each end are 180° out of phase. This same deflection pattern was observed at 279.123 Hz (Figure 48) with even less accompanying vertical motion. The last frequency considered is 293.910 Hz. As shown in Figure 49, this is primarily a bending mode in the shape of a sine wave.

Figures 50 thru 62 show the MODAL-PLUS geometry and generated mode shapes, from random excitation data, for some of the low frequency modes of the two structures. Quite a few more modes at low frequency have been easily identified from the 'random' data than for the 'impulse' data.

The Primary Mass geometry was revised to avoid the confusion resulting from too many interconnecting lines in the animation. A cross section (Figure 50) trace permits a simpler animation of the several modes illustrated in Figures 51 thru 56. Note that the geometry was made to include the two points defining position of the Gyro Test Table (GTT) on the SSP, thus providing information on motion of the GTT at the vibration mode frequencies shown.

22

The Secondary Mass geometry, Figure 57, was also limited to a partial structure (data from points on the full figure is in the analysis, and only a simple trace of the results is used in the animation). Figures 58 thru 62 illustrate the animation of the lower frequency modes.

Some caution is required in deciding which of these several modes are most important. Relative amplitudes of modes are important; however, amplitude comparisons are valid only if the same response point was used for PCALC of both resonances. The Bode plot is best for amplitude comparisons. Another important measure of the resonance is the damping coefficient. A very heavily damped resonance may be difficult to locate, and of little consequence as a structural resonance effect on the controls system. Examples of these two considerations may be seen from the SSP Primary Mass Parameter File (Table 5). The 142 Hz mode has a far greater effect than the lower modes at 120 and 95 Hz. The amplitudes values are comparible, 2:1 and 3:1 respectively, but the 142 Hz calculation is not based on data from the same response point as the 120 and 95 Hz modes. Also, it should be noted that the damping coefficients of the 120 and 95 Hz modes are much larger than that of the 142 Hz mode. A third factor important to the controls development is the mode shape as it relates to the proposed location of sensors and actuators. For example, the 4th mode at 40.5 Hz is small amplitude and moderately damped; however, the mode shape is such that maximum motion of this resonance is at the very point where it is proposed to locate a vertical shaker and sensor (Figure 51).

In the example just given, when the reference and response points taken correspond to the contractor's suggested locations for South vertical shaker and sensor respectively, the 40.5 Hz mode acceleration is -40 db down from the principle, 142 Hz mode, and consequently, the 40.5 Hz mode is probably insignificant to the control design. To minimize structural dynamics effects on the control system, the possible effect of each mode must be considered in the selection process of sensor and actuator locations, a task in the follow-on SSP development effort.

10.6 SSP Design Verification

Table 6 shows actual (MODAL-PLUS) vs theoretical (contractors Stardyne analysis) values for the lower resonance modes. It is evident

23

from Table 6 that the experimental and finite element results do not correspond. These are very complex structures and care must be taken to compare results for the same mode. This wasn't done; rather, the important criteria of <u>lowest resonances</u>, damping, and mode shape were the main considerations. Some comparison by mode undoubtedly is in order. However, as far as lowest resonances, the SSP controls development certainly must take account of resonances at lower frequencies than intended during the structural design phase.

Table 6. SSP Natural Frequencies (Hz)

MASS	MODAL-PLUS (RANDOM EXCITATION)	THEORETICAL (STARDYNE)
Primary	40,61,87,95, and 120 (small AR)*	119
Primary	142 (large AR)	155
Primary	253 (large AR)	186
Secondary	22,50,62, and 90 (small AR)	–
Secondary	101 (large AR)	118
Secondary	278 (large AR)	230
Secondary	380 (large AR)	–

* AR: Amplitude Ratio

11. CONTROLS ANALYSIS OF THE SSP TWO-STAGE SYSTEM

Due to concerns about the feasibility of controlling the SSP, a theoretical study of possible control techniques was conducted in July and August 1981 by Lt Murphy. His study began with a review of the model for the SSP, a determination of controlability and observability, a preliminary design of a classical control system, and finally, tests to try to experimentally determine the SSP transfer function.

Figure 63 is a schematic of the dynamic model used by MAC and Lt Murphy for determining transfer functions. The masses for these models are based on the values given in the MAC final design report. The constants for the spring and damping coefficients were derived from data given in the final design report on tests of the pneumatic isolators.

A block diagram of the vertical translation characteristics for the above system can be drawn as shown in Figure 64. From this model, transfer functions can be easily derived for several important relations:

24

$$\frac{z_2}{z_0} = \frac{\text{Position of Primary Mass}}{\text{Position of Pier}}$$

This is the passive transmissivity of the isolation system.

$$\frac{z_2}{F} = \frac{\text{Position of Primary Mass}}{\text{Actuator Forces to Primary Mass}}$$

This is the transfer function which will be used in actively controlling the system's vertical motion.

Using Mason's Loop Rule[10] one can show that the denominator of all three expressions are identical and equal to:

$$\Delta = m_1 m_2 s^4 + (m_1 f_2 + m_2 f_1 + m_2 f_2) s^3 +$$
$$(m_1 k_2 + m_2 k_2 + m_2 k_1 + f_1 f_2) s^2 +$$
$$(f_1 k_2 + f_2 k_1) s + k_1 k_2$$

Substituting values given in Figure 63, one finds that the poles of the system are both lightly damped second-order complex pairs with the following characteristics:

Natural frequency (ω_n):	8.39 R/S	26.4 R/S
Equivalent Hertz :	1.34 Hz	4.20 Hz
Damping Ratio ($\S$) :	.022	.070

For the transfer function $\dfrac{z_2}{z_0}$, the resulting numerator is:

$$N_1(s) = f_1 f_2 s^2 + (f_1 k_2 + f_2 k_1) s + k_1 k_2 = (f_1 s + k_1)(f_2 s + k_2)$$

This provides two zeros with identical coner frequencies of 189 R/Sec = 30 Hz. A plot of this theoretical isolation capability is shown in Figure 65. When desired transmissivity characteristics are superimposed on this plot, we find that the response at high frequencies is adequate, but that to attain the required transmissivities at lower frequency, an active control system is indicated. We should also note that the theoretical roll-off of this system is the desired 80 dB/decade for only a small frequency range around 10 Hz due to the real zero located at 30 Hz.

For controlling the system in translation we must concern ourselves with the transfer function $\dfrac{X_2}{F}$. The numerator term for this transfer function is:

$$N_2(s) = m_1 s^2 + (f_1 + f_2)s + (k_1 + k_2)$$

Using given values results in a complex zero with $\omega_n = 25.289$ R/Sec
(4.02 Hz) and $\S = .067$. To check for controllability and observability,
the equations must be rewritten in state variable form. As a first step
in doing this we will rewrite the transfer function, $\dfrac{X_2}{F}$, as

$$\frac{Z_2}{F} = \frac{K(s^2 + b_1 s + b_0)}{s^4 + a_3 s^3 + a_2 s^2 + a_1 s + a_0}$$

where: $k = \dfrac{1}{M_2}$ $\qquad K = \dfrac{1}{M_2}$

$$a_0 = \frac{K_1 K_2}{M_1 M_2} \qquad\qquad b_0 = \frac{K_1 + K_2}{M_1}$$

$$a_1 = \frac{F_1 K_2 + f_2 k_1}{M_1 M_2} \qquad\qquad b_1 = \frac{f_1 + f_2}{M_1}$$

$$a_2 = \frac{M_1 K_2 + M_2 K_2 + M_2 K_1 + f_1 f_2}{M_1 M_2}$$

$$a_3 = \frac{M_1 f_2 + M_2 f_1 + M_2 f_2}{M_1 M_2}$$

The general form of the equation in state variable form is:

$$\dot{\bar{X}} = F\bar{X} + G\bar{u}$$

Where $\bar{X}$ is vector of four components, F a 4x4 state matrix, u the scalar
input, and G a 4x1 control matrix. The output of the system is a linear
combination of the state and is described by the measurement equation:

$$\bar{y} = H\bar{x}.$$

For this system, MAC proposes a seismometer with both position and
velocity pick-offs. Therefore, our measurements would be

$y_1 = Z$ = position of primary mass

$y_2 = \dot{Z}$ = velocity of primary mass

Given a system transfer function, there are a limitless number of defini-
tions of the states, X, and associated state and measurement equations
which model the system. To easily check controllability and observabil-
ity, two standard forms make the process easy: For observability we use
the observer canonical from where:

$$F = \begin{bmatrix} -a_3 & 1 & 0 & 0 \\ -a_2 & 0 & 1 & 0 \\ -a_1 & 0 & 0 & 1 \\ -a_0 & 0 & 0 & 0 \end{bmatrix} \qquad G = \begin{bmatrix} 0 \\ 0 \\ b_1 \\ b_0 \end{bmatrix}$$

$$H = K \begin{bmatrix} 1 & 0 & 0 & 0 \\ -a_3 & 1 & 0 & 0 \end{bmatrix}$$

To show observability we must show that the rank of the matrix:

$$\begin{bmatrix} H \\ HF \\ HF^2 \\ HF^3 \end{bmatrix} , \qquad \text{is at least four.}$$

When we form this 8X4 matrix we find that the rank is four and, therefore, the system is observable.

For checking controllability, we use the control canonical form where:

$$F = \begin{bmatrix} 0 & 1 & 0 & 0 \\ 0 & 0 & 1 & 0 \\ 0 & 0 & 0 & 1 \\ -a_0 & -a_1 & -a_2 & -a_3 \end{bmatrix} \qquad , \qquad G = \begin{bmatrix} 0 \\ 0 \\ 0 \\ K \end{bmatrix}$$

$$H = \begin{bmatrix} b_0 & b_1 & 1 & 0 \\ 0 & b_0 & b_1 & 1 \end{bmatrix}$$

To show controllability we must similarly show that the 4X4 matrix $[G \quad FG \quad F^2G \quad F^3G]$ is of rank 4. We again find that the rank is four. Therefore, the system is controllable.

A classical control loop was designed to see if the desired isolation could be obtained on the primary mass using the available signals, Z_2, Z_2 and classical compensators. Figure 66 below provides a vizualization of the system modeled to this point and the control scheme investigated.

Where Δ, $N_1(s)$, $N_2(s)$ were previously defined and:

G_A — Electromagnetic actuator

G_C — Compensator

G_S — Sensor = Seismometer

The first step in the compensation design was to assume that the actuator was just a gain, K_A, and that the seismometers provided measurements of position and velocity, i.e.,

$$G_A = K_A, \quad G_S = (K_p + K_V S)$$

With these two assumptions, it was quite easy to design a compensator. We found that $G_C = K$, that is proportional control was sufficient (assuming we could vary K_p and K_V since they are two separate outputs). This provided very satisfactory performance except a very high gain was required. Further study of this was stopped since it was idealistic at best not to consider the actuator and seismometer dynamics.

The next step in the analysis was to model the seismometer and actuator as follows:

$$G_A = \frac{K_A}{\dfrac{s^2}{\omega_A^2} + \dfrac{2\S_A}{\omega_A} s + 1} \quad ; \quad G_S = \frac{K_1 S^3 + K_p S^2}{\dfrac{s^2}{\omega_S^2} + \dfrac{2\S_S}{\omega_S} S + 1}$$

where: $\omega_A = 2$ (25 Hz) $\qquad \S_A = .7$

$\omega_S = 2$ (.1 Hz) $\qquad \S_S = .707$

We again designed a pseudo-classical compensator consisting of two *proportional plus integral (PI)* compensators and used position, velocity, and acceleration feedback from the sensors. We called this pseudo-classical since with the seismometer, acceleration is not available; we also found that is not observable with only seismometer measurements. However, an accelerometer could be added as a sensor and provide this signal. With this compensator we obtain satisfactory performance, but did not fine tune nor present in detail the results since all the design work was based on an analytical model.

At this point we had an opportunity to take measurements on the SSP at Holloman AFB. A series of seven tests were conducted on 24-25 August 1981 by Mr. Simmons and Lt Murphy of FJSRL with the assistance of Holloman AFB personnel. Preliminary analysis of the data was made by Mr. Simmons and documented in a letter dated 9 Sep 81.

28

His preliminary analysis pointed out that the low frequency vertical behavior due to actuator inputs could be characterized as a complex pole pair resonance at 1.2 Hz followed by a pair of complex zeros and poles at about 3.5 Hz. This agrees in form with the theory where there is a low frequency complex pole pair at 1.34 Hz followed by a complex zero pair at 4.07 Hz and a complex pole point at 4.20 Hz. This data tends to confirm the analytical form of the model with just some specific values being different.

Also identified by these tests were resonances in the response at 95 and 101 Hz. The 101 Hz had been previously identified as the fundamental resonance in the secondary mass, but the source of other resonances was uncertain until analysis by MODAL-PLUS of the random excitation data (see 10.5).

In summary, the data gathered is very good and provides a basis for validating the analytical model which was developed. By using curve fitting techniques, the actual parameters of the SSP can be established and used for further analysis. Analyses planned include the design of a control loop using classical techniques, the investigation of how adding sensors and actuators affects controllability and observability, and finally the design of an optimal control law using full state feedback. Before publication of this document, the SSP analysis was completed, and is being presented to the 1982 AIAA Guidance and Control Conference in August.[10].

12. OTHER SUPPORT TASKS

The various support-to-HAFB tasks that have been provided during the project are documented by R&D Record Book, interim reports, letters, trip reports, viewgraphs, 16 mm film, etc. The reader is referred to the 2304-F2-66 Work Unit file for details of these support tasks; the following is a list of the more important items in this category:

    a. Special Seismic Tests at USAF Academy and Holloman Air Force Base.

    b. Two-Stage System Experimental Simulation

    c. STARDYNE-to-NASTRAN Translation (incomplete)

    d. Design Reviews

    e. Consultation on Systems and Instrumentation

13. CONCLUSIONS

A number of tasks have been accomplished within the work unit scope. These tasks can be summarized as follows:

a. The capabilities were attained at the USAF Academy for experimental and theoretical modeling of complex structures.

b. The experimental modeling technique as applicable to simple and complex structures was verified.

c. The theoretical model technique (by NASTRAN) as applied to a complex structure by comparison to an actual, experimental model was verified.

d. The actual dynamic model of the Holloman SSP for comparison to design specifications was obtained and provided to HAFB.

e. The actual SSP assembly was used to obtain experimental response data as input to the active control system analysis. A control analysis and system model was provided to HAFB.

f. The instructional capabilities of the USAF Academy in the area of dynamic analyses were significantly enhanced.

In the process of providing verification of structures analysis techniques and the controls analysis, presentations have been made (or scheduled) to 1981 AIAA G&C,[6] 1982 AIAA G&C,[9] Bidders Conference on further SSP development, University of New Mexico State Engineering Department, and the 1st International Modal Analysis.[11]

It is concluded that all of the work unit objectives, see Section 3, were met. Additionally, certain detail conclusions were reached regarding the prototype SSP. These details have been provided within this and other referenced documents to HAFB. Most important among these findings are the following: the original specifications for structural behavior are very important to the system control model, and these specifications were not met; the resultant SSP transmissibility does not roll-off with the desired -80 db/decade rate but can be controlled, in the vertical axis investigated, to the prototype requirements; and the prototype SSP can be made a satisfactory test base in the 10^{-8} g stability regime, and a valuable and necessary step in the long range objective of developing a 10^{-9} g stable inertial instrument test platform.

Finally, it is our opinion, seconded by Holloman AFB, that this
support effort was crucial to the development of the prototype SSP and
the Air Force's capability for testing of a new generation of inertial
navigation instruments.

14. RECOMMENDATIONS

As this support effort came to a close, the 'passive' SSP system had
been designed, fabricated, and installed at Holloman AFB's Advanced
Inertial Test Laboratory. As plans were developed at HAFB for continued
development of the system, first the instrumentation, then active
controls, some problems were identified. Two problems identified were
non-conformity of the structural behavior with contractor specifications,
e.g., low frequency resonance, and deviation of high frequency trans-
missibility roll-off from the 'theoretical' expectations. These problems
were clarified in this support effort, and the potential for solutions
established. As the development of the SSP continues, other problems may
arise which have potential for solution within the expertise of FJSRL and
the faculty of the USAF Academy.

It is recommended that the need for a special test environment for
new, more precise, guidance equipment be recognized as the beyond state-
of-the-art, research problem that it is, and that support to HAFB's
spearhead research project in a quieter motion environment test base, be
continued.

15. ACKNOWLEDGEMENTS

16. APPENDIX A

MODAL PLUS Program Routines

1. FILEM (File Manipulation) - This sub-program must always be run first. The FILEM routine creates files to store all required data for new projects or brings old files from disc storage to active memory for continued or new work.

2. GEOM (Geometry) - The geometry routine lets the user select a coordinate system and model his structure as desired. The geometry points must be set up if the user wishes to take data at specified points on the structure. It is important to remember that the number of geometry points will equal the number of points at which data must be collected.

3. LOCTR (Location Trace) - Connects all of the geometry points with a solid line trace as the user directs. Without the location trace the program would be unable to give a dynamic display of the mode shapes. It is also possible to divide one's structure into more than one trace for simplicity.

4. GEOPRE (Geometry Preview) - Allows the user to view a static picture of his structure as defined by his work in GEOM and LOCTR. It is primarily a visual check to insure that no mistakes have been made in the initiation of 2. and 3. above.

5. SETCON (Set Conditions) - Allows the user to specify the test conditions such as sample size, maximum frequency, maximum voltage, etc. This program must be run before DATAQ (below). An oscilloscope is helpful in determining the voltage levels of the input signals.

6. DATAQ (Data Acquisition) - This routine takes inputs both in the form of acceleration and force and plots an acceleration over force (A/F) curve, or transfer function, on a Bode diagram. The program also allows one to view sample signals of the input data to make sure that all test conditions are adequate and that proper data is being obtained. This part of the program is the major component of 'MODAL PLUS'. Acceleration data must be taken at all non-fixed points while impact data is always taken at one non-fixed point (fixed points are ones that do not move). The quality of data received here affects the rest of the modal analysis.

32

7. PCALC (Parameter Calculations) - PCALC allows the user to select resonant peaks from the Bode diagrams in DATAQ for computer calculations of damping coefficients, phase, amplitude, frequency, etc. Resonant peaks usually correspond to 180 degree phase shifts.

8. SCALC (Shape Calculations) - This routine calculates the modal coefficients of each geometry point for a selected resonance and must be run after PCALC. Two calculation methods are available. The total response calculation is fast but less accurate with no user control, whereas the single degree of freedom fits (or circle fits) of each geometry point is slower but more accurate and can be controlled by the user.

9. ANIMAT (Animation) - ANIMAT is only run after GEOM and LOCTR have been defined and PCALC and SCALC have been calculated. ANIMAT is the culmination of the 'MODAL PLUS' program. It displays the structure's mode shapes dynamically at selected resonant frequencies.

17. REFERENCES

1. DiPaola, R., Kochakian, C.R., and Tsutsumi, K., "Geokinetic Considerations for Advanced Testing of Gyros and Accelerometers," AIAA Paper 75-1066, AIAA Guidance and Control Conference, August 1975.

2. Lorenzini, Dino A., "Active Control of a Pneumatic Isolation System," AIAA Paper 72-843, AIAA Guidance and Control Conference, August 1972.

3. Whitesell, W.J., and Hooten, T.R., "Progress and Plans for the Development of a Precision Guidance Test Facility," CIGTF Symposium, Holloman AFB, NM, Oct 1979.

4. Simmons, Bill J., "Seismic Motion Stability, Measurement, and Precision Control," Final Report, SRL-TR-79-0015, F.J. Seiler Research Laboratory, USAF Academy, CO, Dec 1979.

5. Martelli, V.P., Watkins, D.R., and Klein, G. Harold, "Nano-G Stable Platform Design," AIAA Paper 81-1815, AIAA Guidance and Control Conference, Aug 1981.

6. Simmons, B.J., Hanes, R.M., and Heming, F.S., Jr., "Dynamic Analysis of Test Platform," AIAA Paper 81-1816, AIAA Guidance and Control Conference, Aug 1981.

7. Broderson, Emil, "Stabilization of a Seismic Isolation Block, Inertial Instrument Testing," AIAA Paper 74-857, AIAA Guidance and Control Conference, Aug 1974.

8. Harris, C.M., and Crede, C.E., Shock and Vibration Handbook, Second Edition, McGraw-Hill Book Co., 1976.

9. Dorf, Richard C., Modern Control Systems, Second Edition, Addison-Wesley, 1974, p 52.

10. Morgan, Felix E., and Simmons, Bill J., "Stabilization Techniques for the CIGTF Seismically Stable Platform," AIAA Paper 82-1584, AIAA Guidance and Control Conference, Aug 82.

11. Heming, Francis S., Jr., and Simmons, Bill J., "Comparison of Finite Element and Experimental Modal Analyses of a Complex Structure," First International Modal Analysis Conference, Nov 1982.
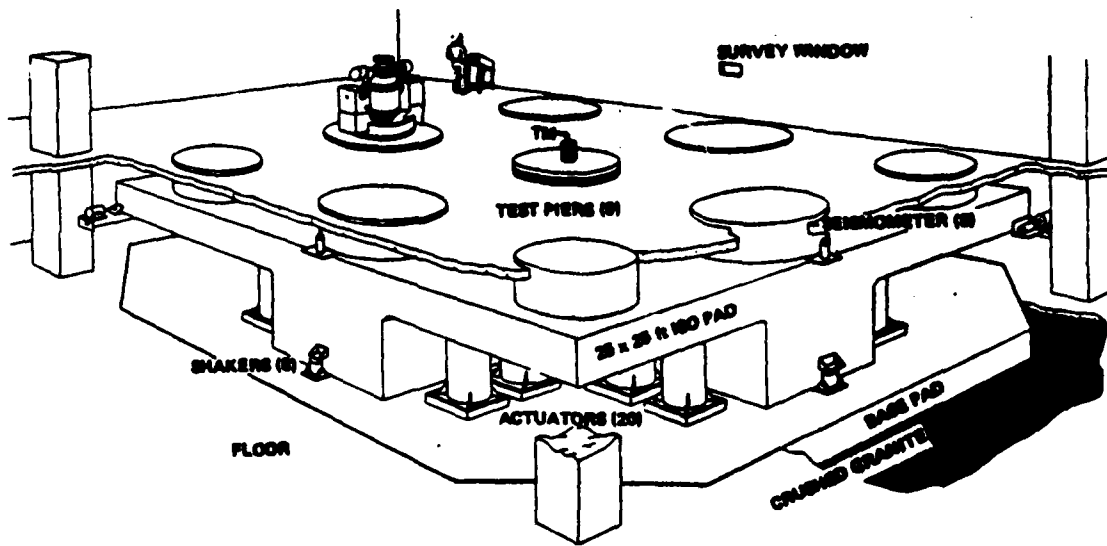
Figure 1. Iso-Pad Pictorial
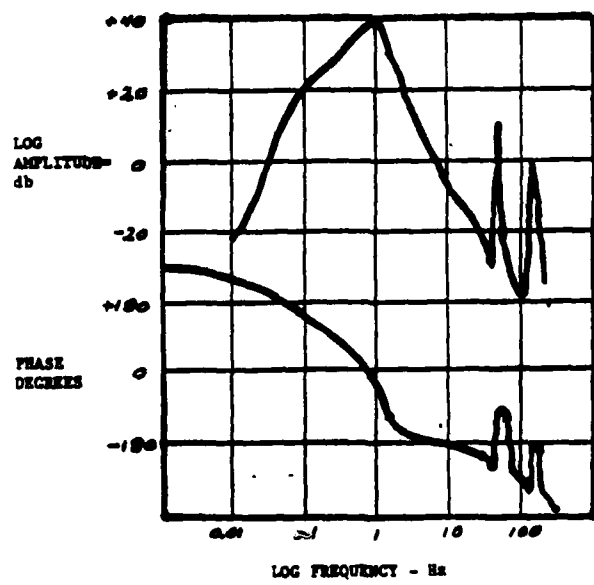
Figure 2. Open Loop Response of Angular Control Loop

35
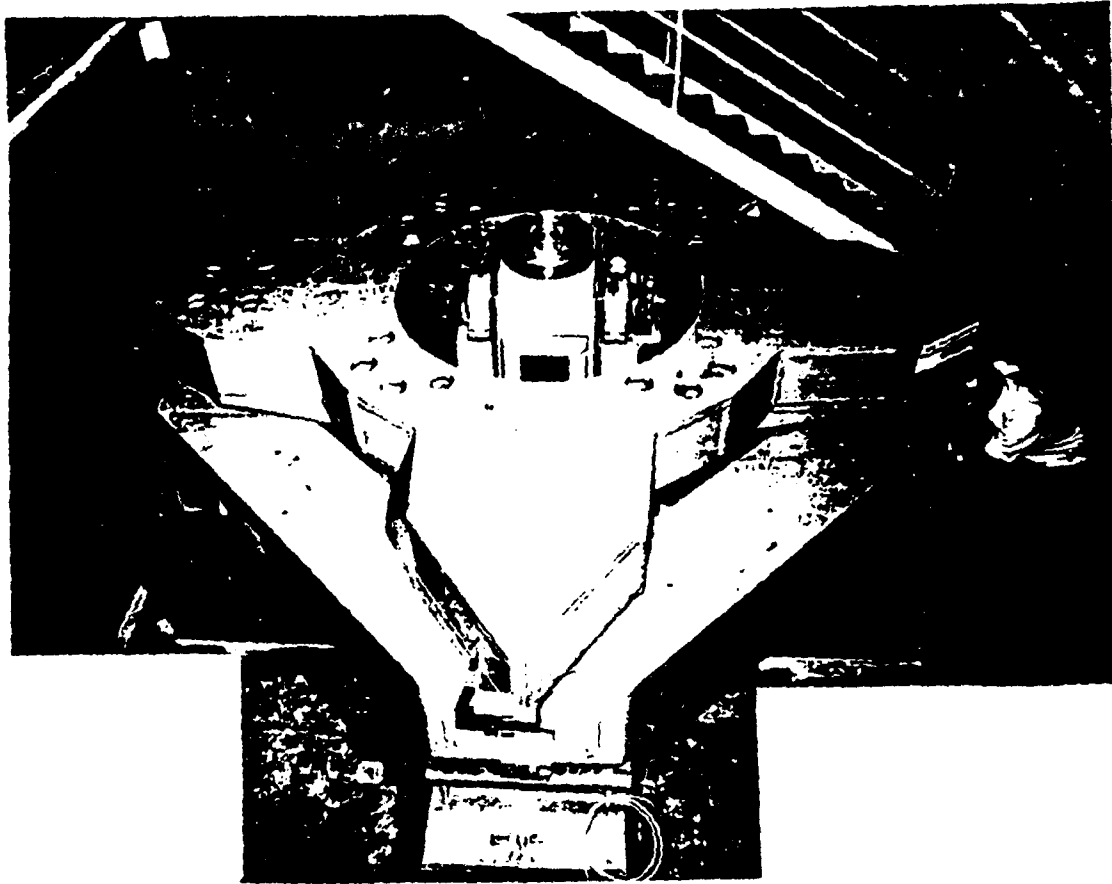
Figure 3. Seismically Stable Platform
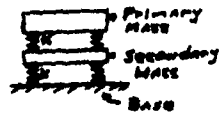
Figure 4. Dual Isolator Schematic
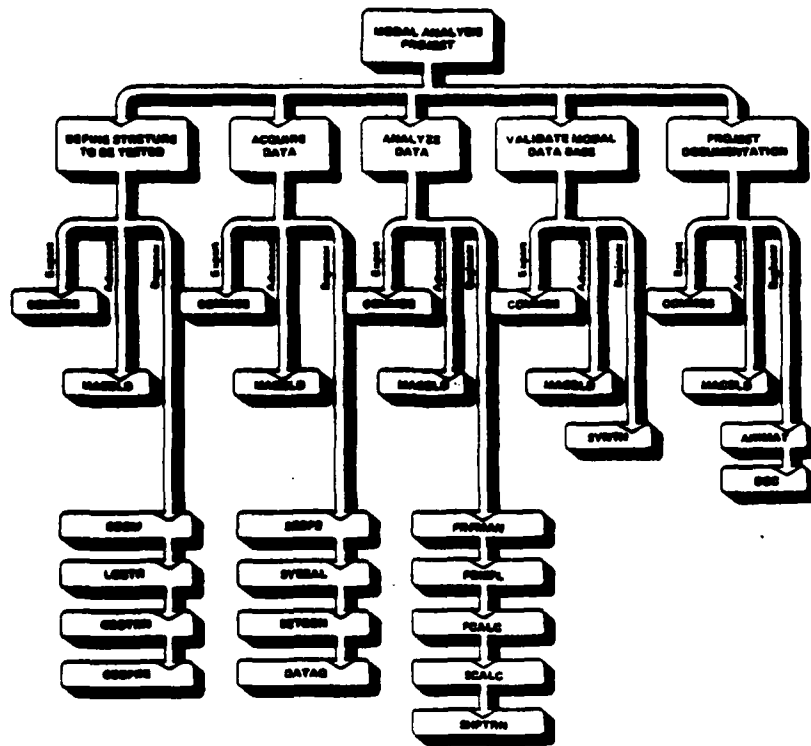
Figure 5. MODAL PLUS Structure
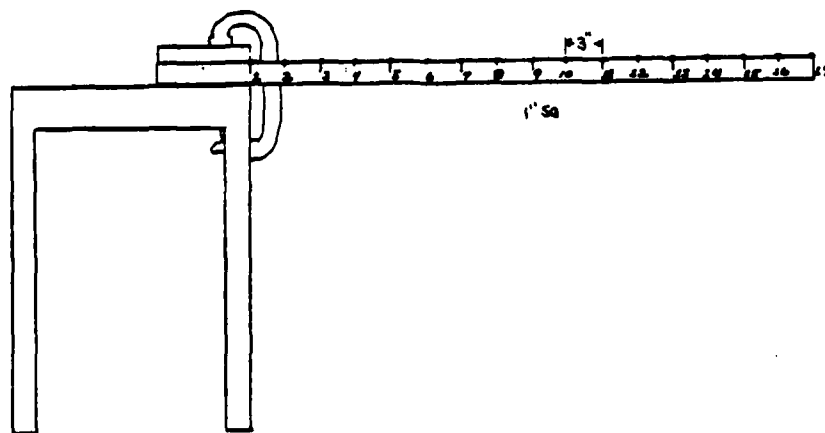
Figure 6. Cantilever Beam

37
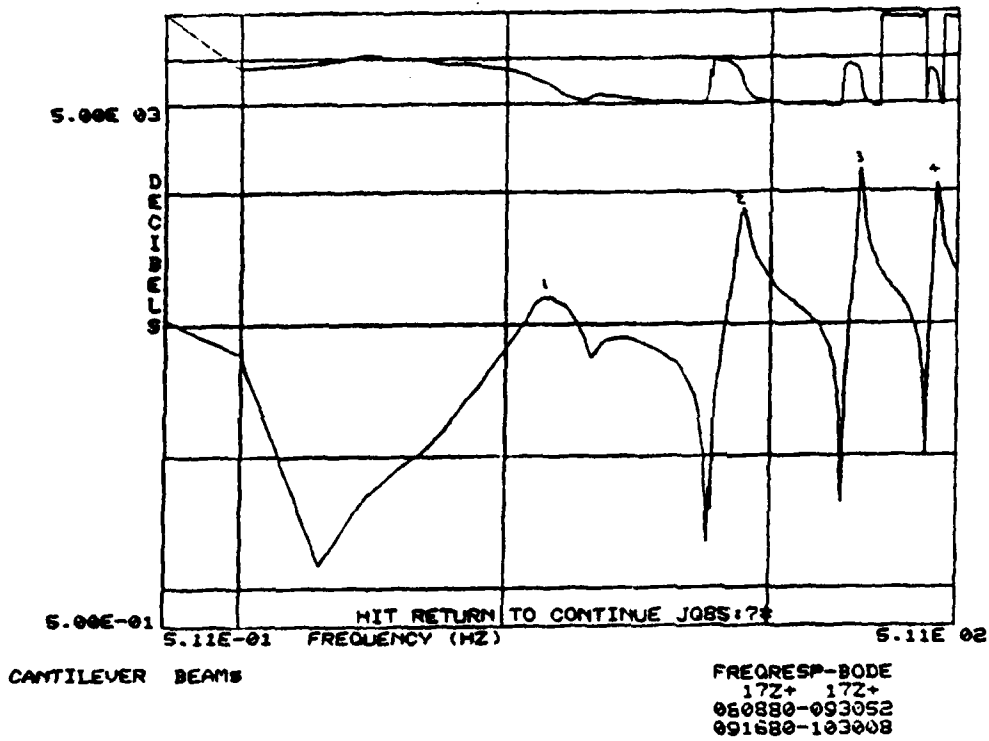
Figure 7. Bode Diagram (Cantilever Beam)
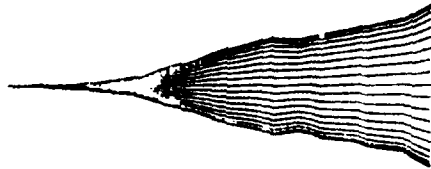
Figure 8. 1st Mode, 12,949 Hz, Cantilever Beam
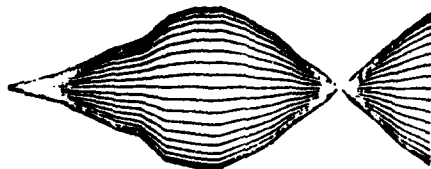
Figure 9. 2nd Mode, 80.304 Hz, Cantilever Beam

38
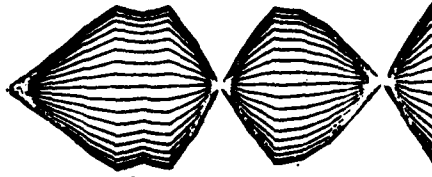
Figure 10. 3rd Mode, 222.369 Hz, Cantilever Beam
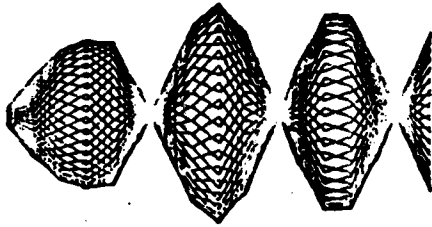
Figure 11. 4th Mode, 433.877 Hz, Cantilever Beam
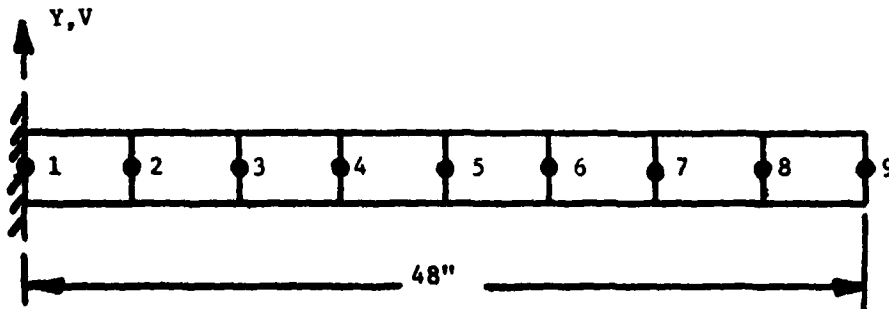
Figure 12. NASTRAN Model, Cantilever Beam
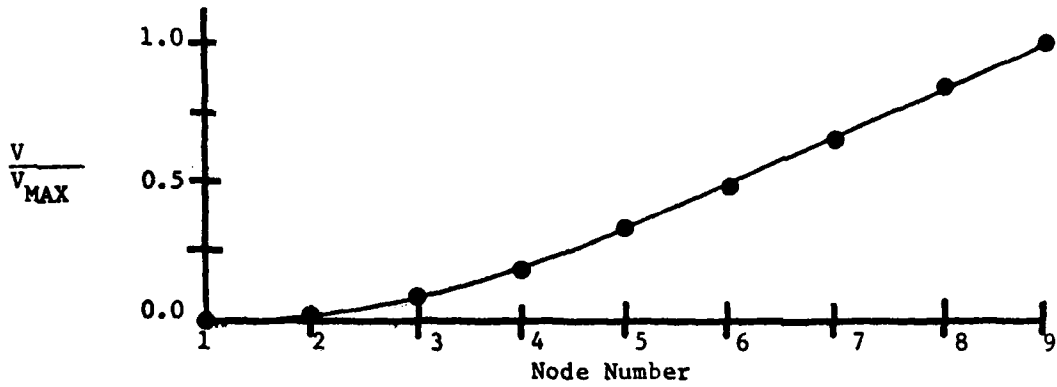
Figure 13. 1st Mode, 13.83 Hz, Beam (NASTRAN)
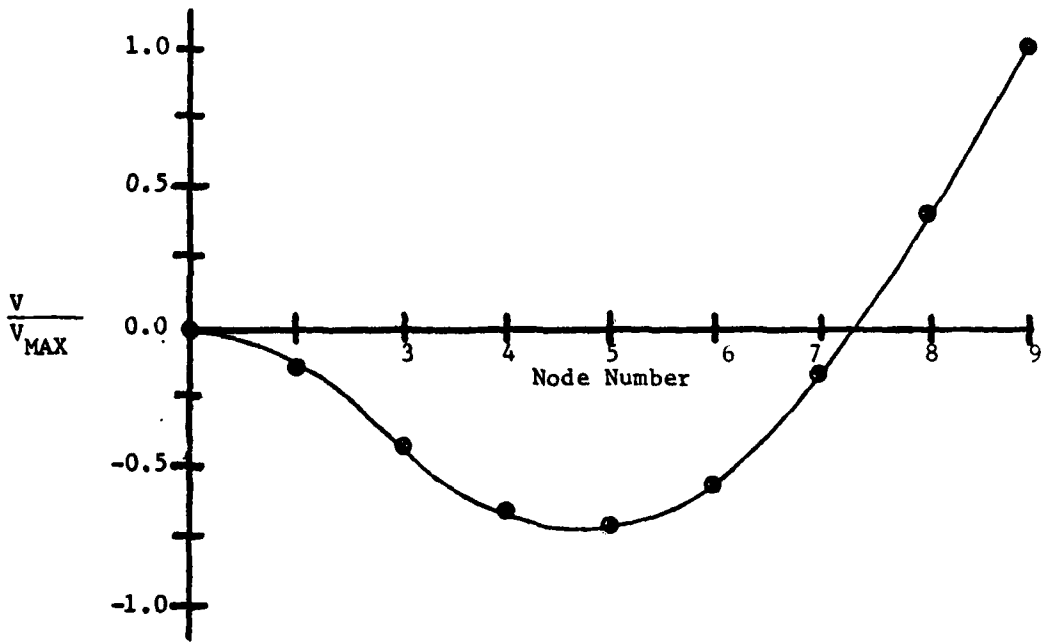
Figure 14. 2nd Mode, 85.07 Hz, Beam (NASTRAN)

40
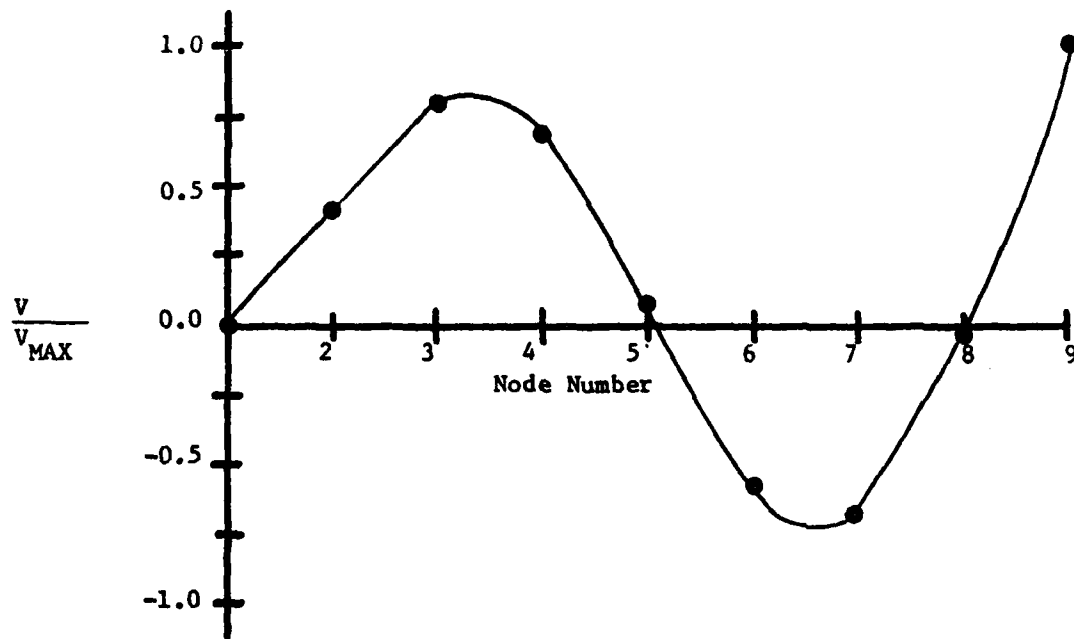
Figure 15. 3rd Mode, 233.94 Hz, Beam (NASTRAN)
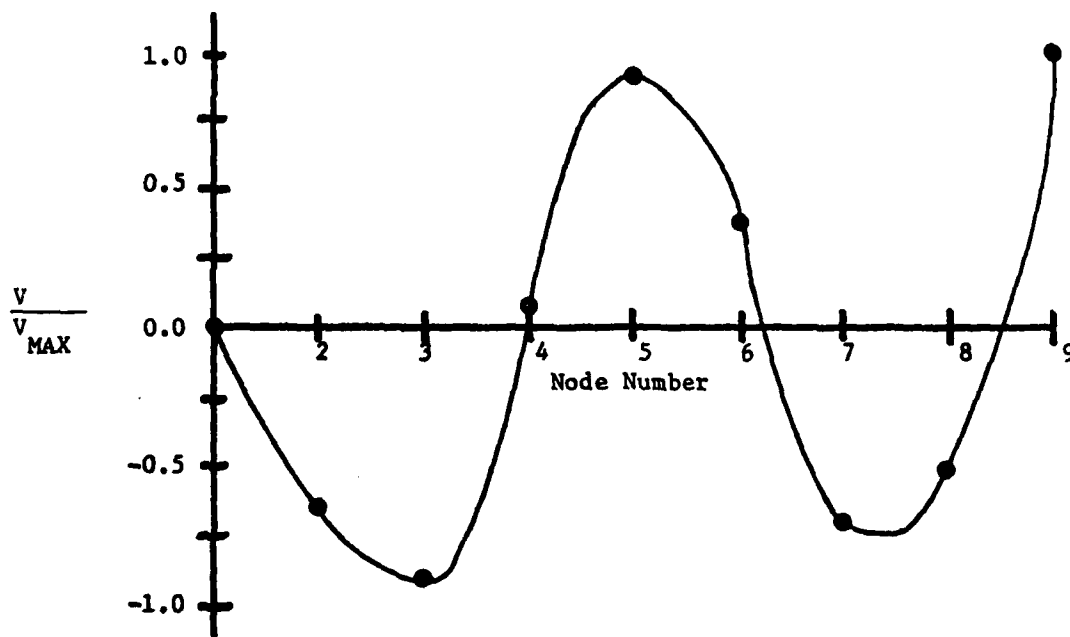
Figure 16. 4th Mode, 449.21 Hz, Beam (NASTRAN)

41
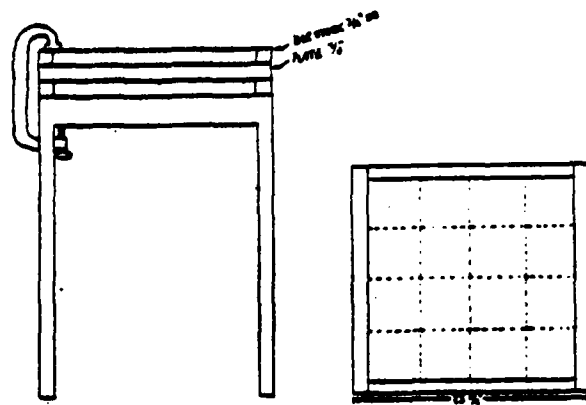
Figure 17.   Square Aluminum Plate
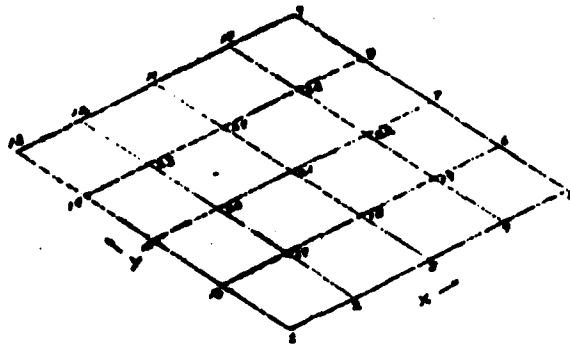
Figure 18.   Plate Geometry
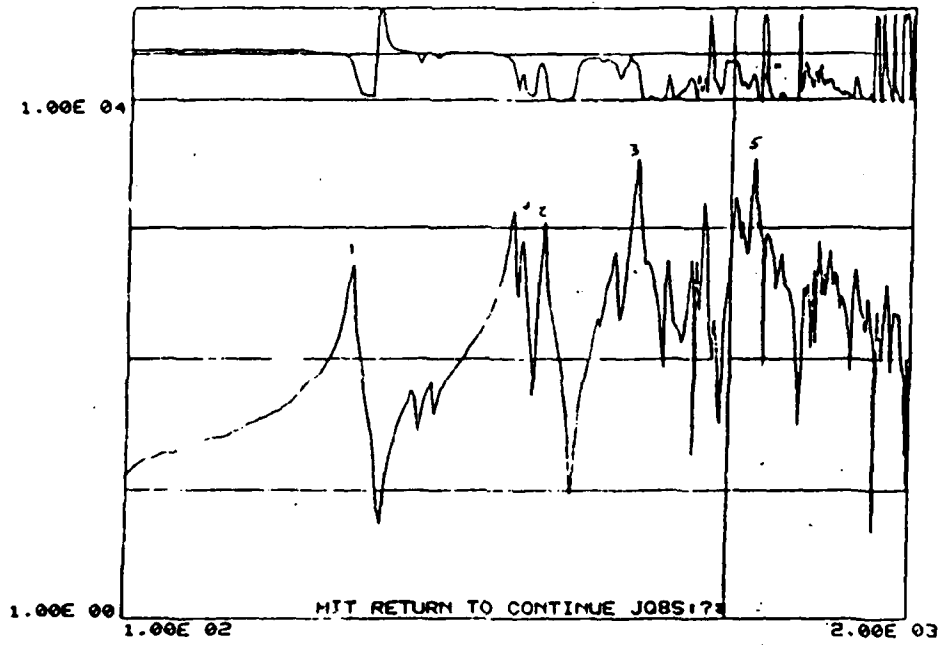
Figure 19. Bode Diagram (Square Aluminum Plate)
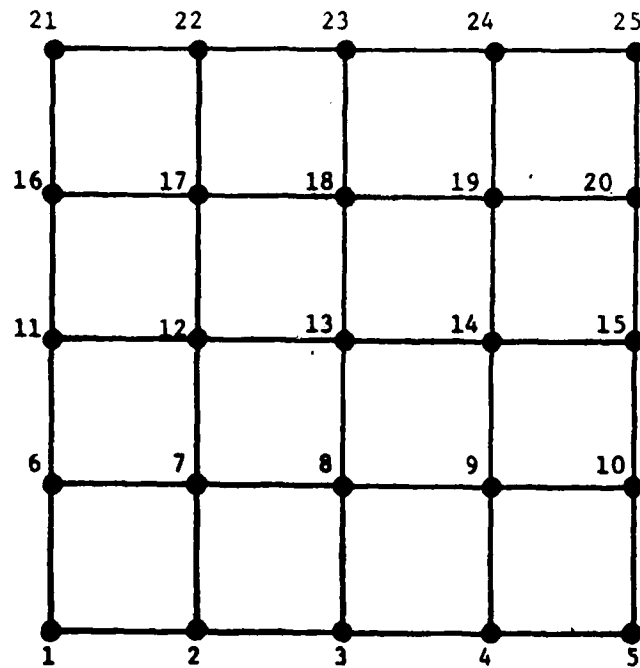
Figure 20. NASTRAN Model, Square Plate

43
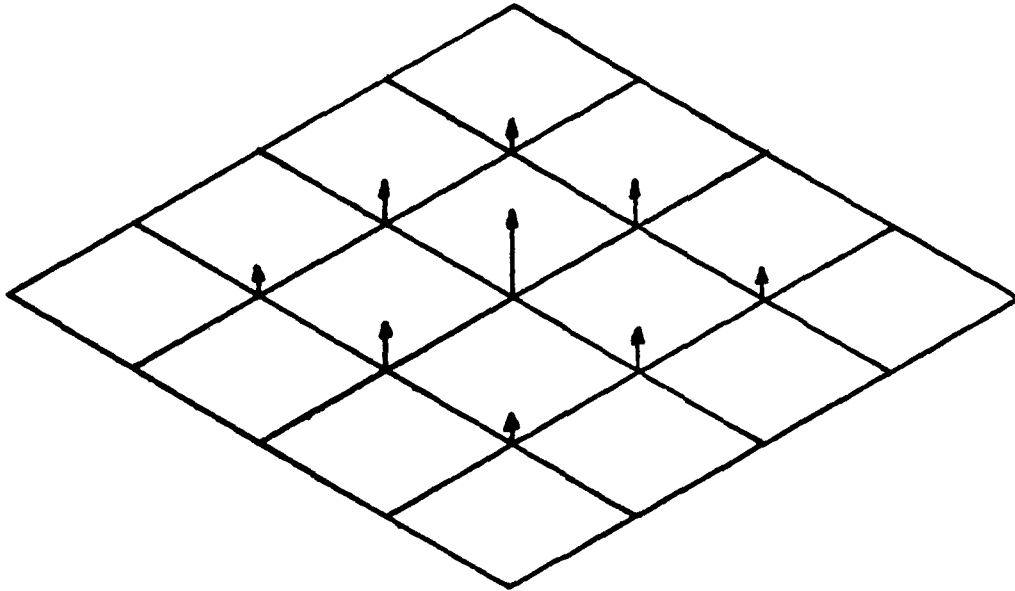
Figure 21. 1st Mode, 259 Hz, Plate (NASTRAN)
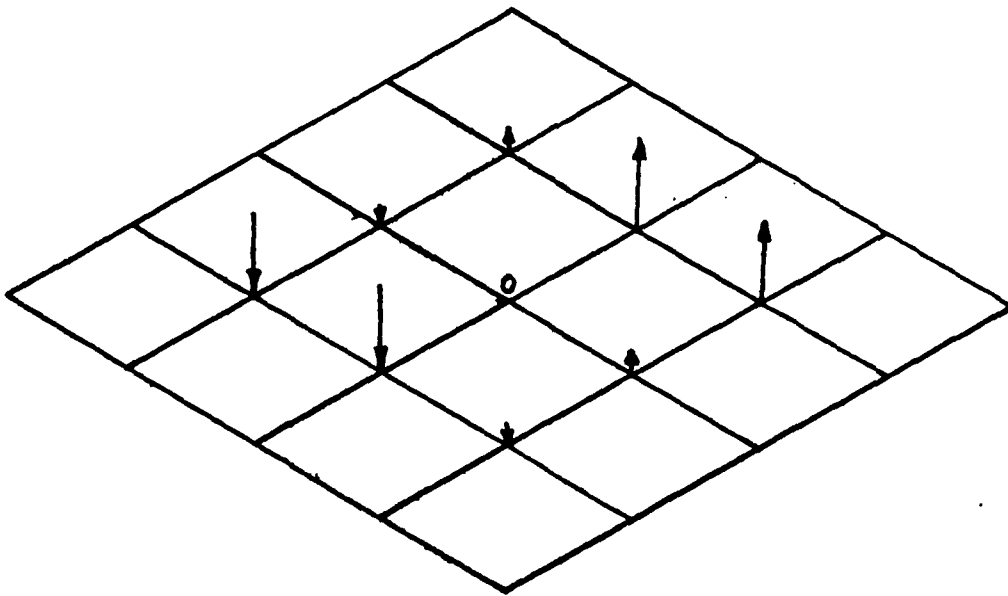
Figure 22. 2nd Mode, 530 Hz, Plate (NASTRAN)

44
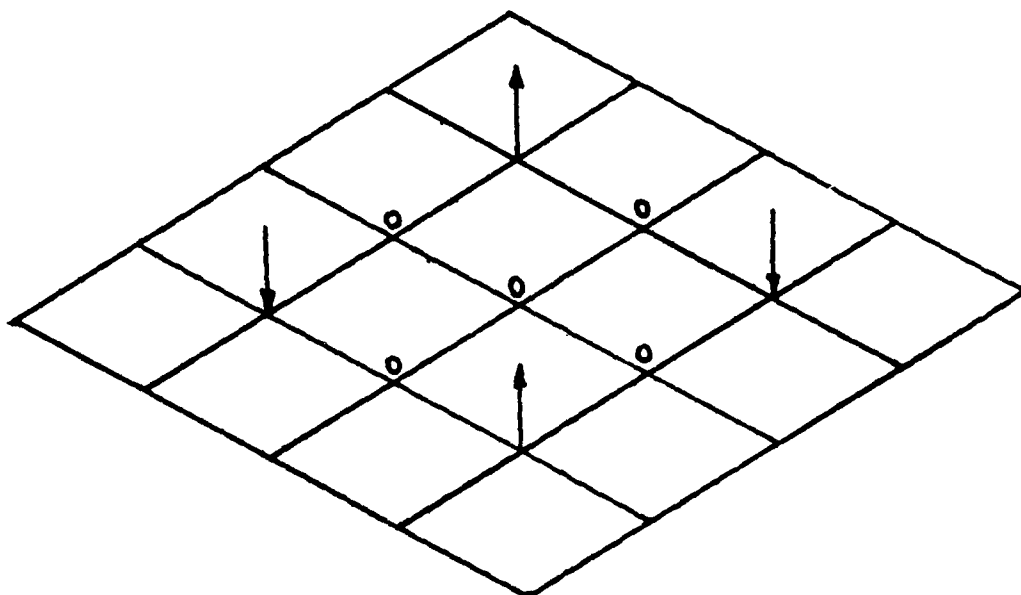
Figure 23.   3rd Mode, 769 Hz, Plate (NASTRAN)
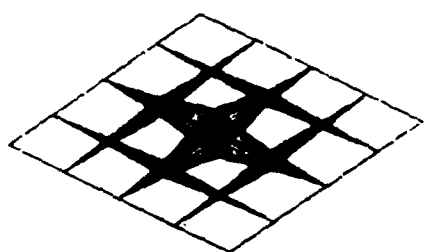
(a) Mode 1, 230 Hz
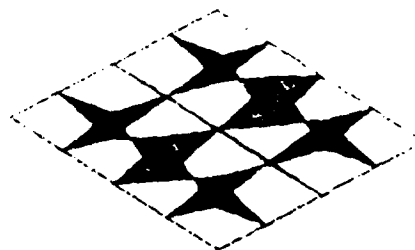
(b) Mode 2, 471 Hz
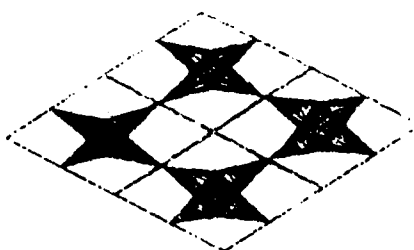
(c) Mode 3, 704 Hz

Figure 24.   Plate Resonant Modes

45
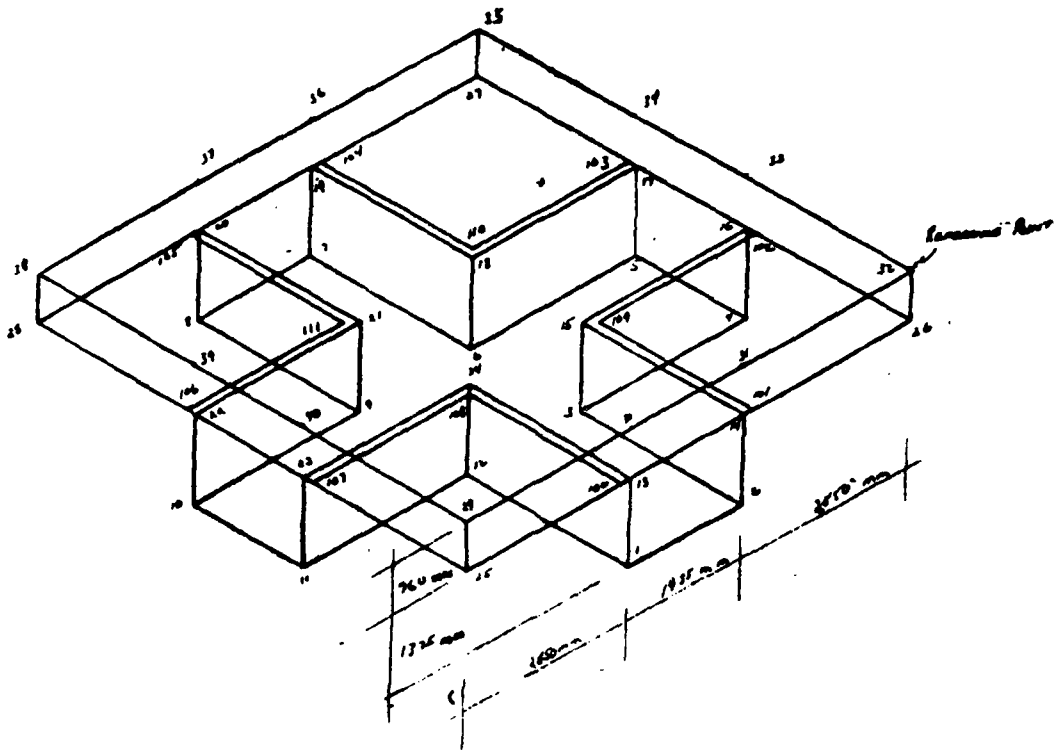
Figure 25. Iso-Pad Geometry

GEOMETRY

LOC	X	Y	Z
1	2850	0	0
2	4790	0	0
3	4790	2850	0
4	7635	2850	0
5	7635	4783	0
6	4790	4783	0
7	4790	7635	0
8	2850	7635	0
9	2850	4790	0
10	0	4790	0
11	0	2850	0
12	2850	2850	0
13	2850	0	1373
14	4790	0	1373
15	4790	2850	1375
16	7635	2850	1375
17	7635	4790	1375
18	4790	4790	1375
19	4790	7635	1383
20	2850	7635	1390
21	2850	4790	1375
22	0	4790	1373
23	0	2853	1370
24	2850	2853	1370
25	0	0	1390
26	7635	0	1390
27	7630	7635	1368
28	0	7640	1365
29	0	0	2135
30	2850	0	2135
31	4790	0	2132
32	7635	0	2132
33	7635	2850	2115
34	7635	4783	2150
35	7630	7635	2120
36	4790	7635	2135
37	2850	7635	2137
38	0	7840	2127
39	0	4790	2131
40	0	2853	2129
100	2700	0	1373
101	4935	0	1373
102	7635	2710	1375
103	7635	4933	1375
104	4945	7635	1383
105	2710	7635	1390
106	0	4940	1373
107	0	2763	1370
108	2700	2763	1370
109	4935	2710	1373
110	4945	4933	1375
111	2710	4940	1373

Figure 26. Iso-Pad Geometry Modal Coordinates

46
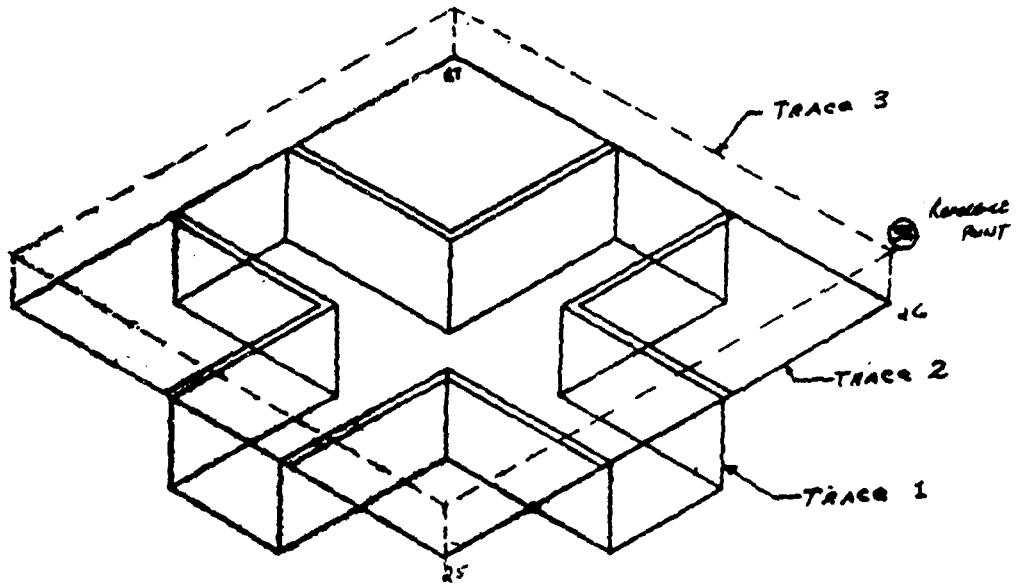
Figure 27.   Iso-Pad Coordinate Traces
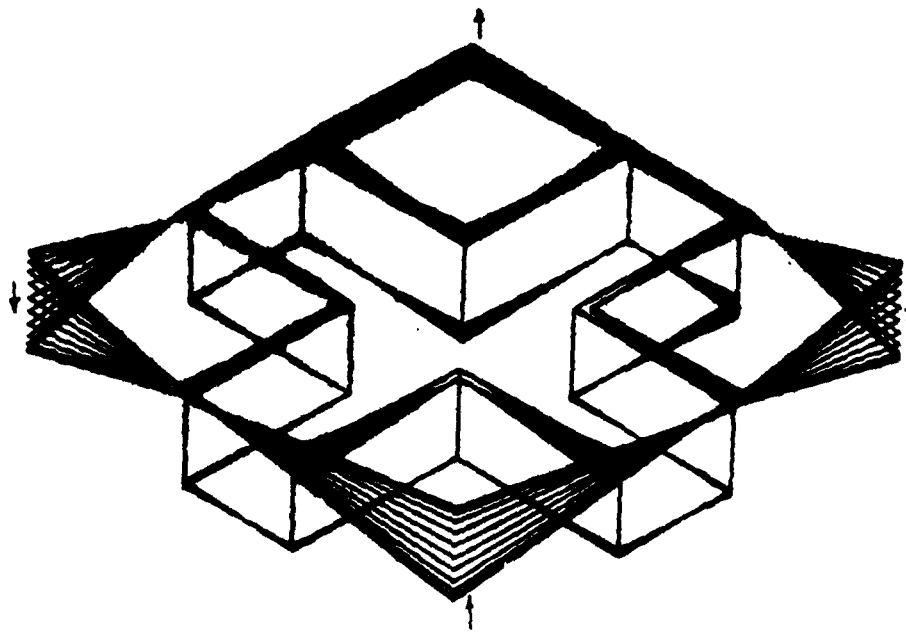
Figure 28.   1st Mode, 46.412 Hz, Iso-Pad

47
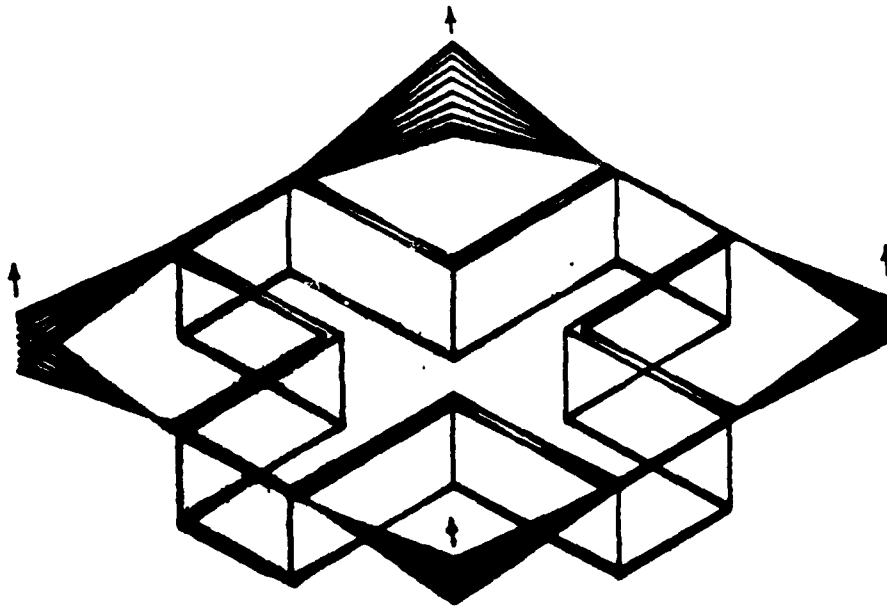
Figure 29. 2nd Mode, 57.408 Hz, Iso-Pad
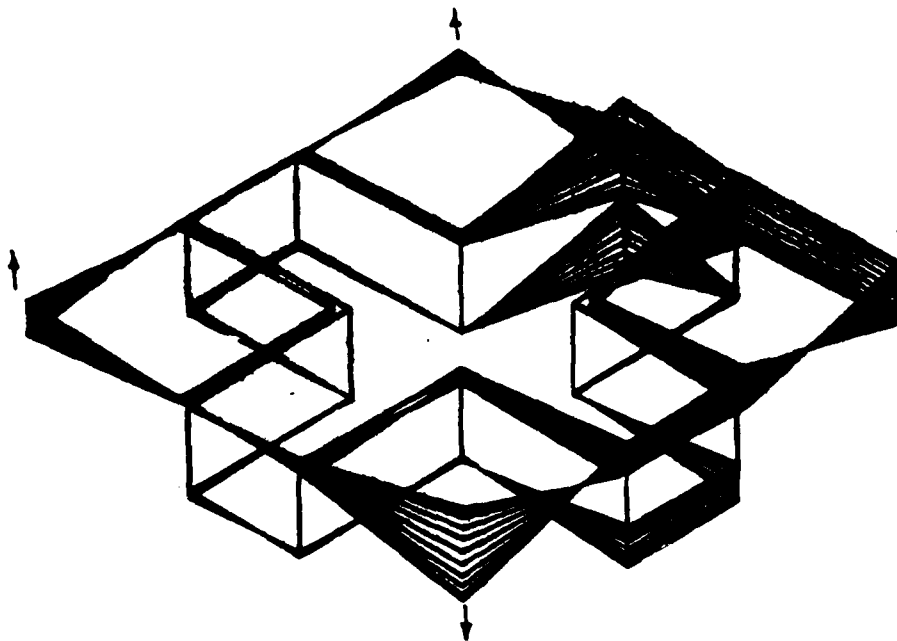
Figure 30. 3rd Mode, 66.923 Hz, Iso-Pad

48
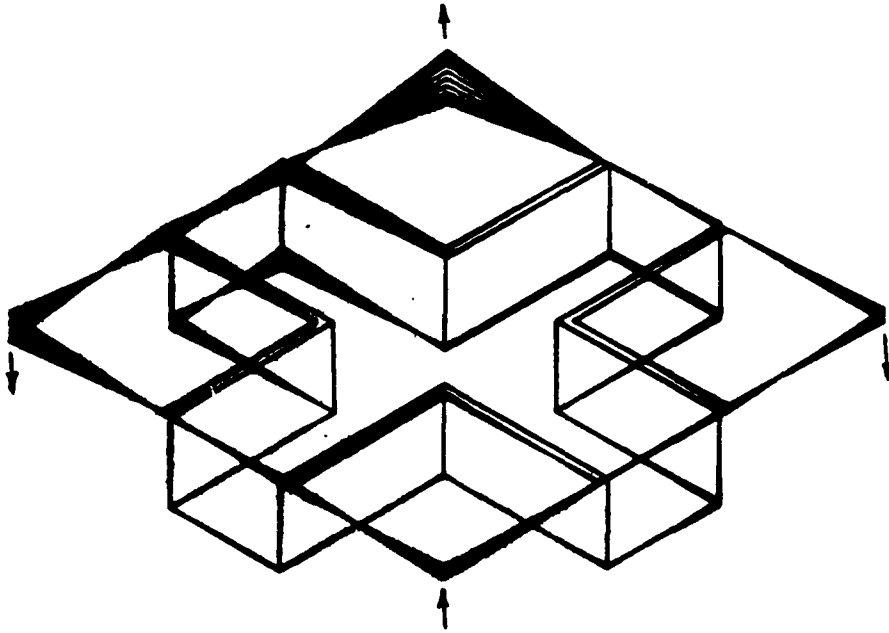
Figure 31. 4th Mode, 120.919 Hz, Iso-Pad
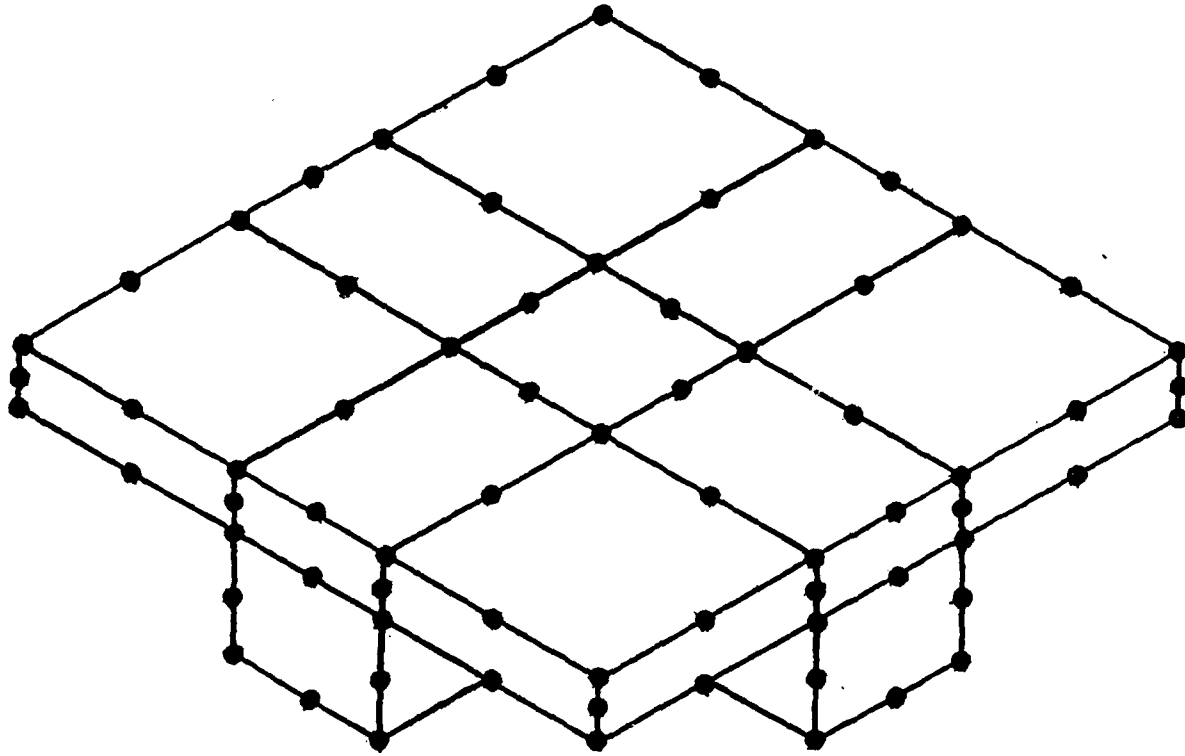
Figure 32. NASTRAN Whole Structure Model, Iso-Pad
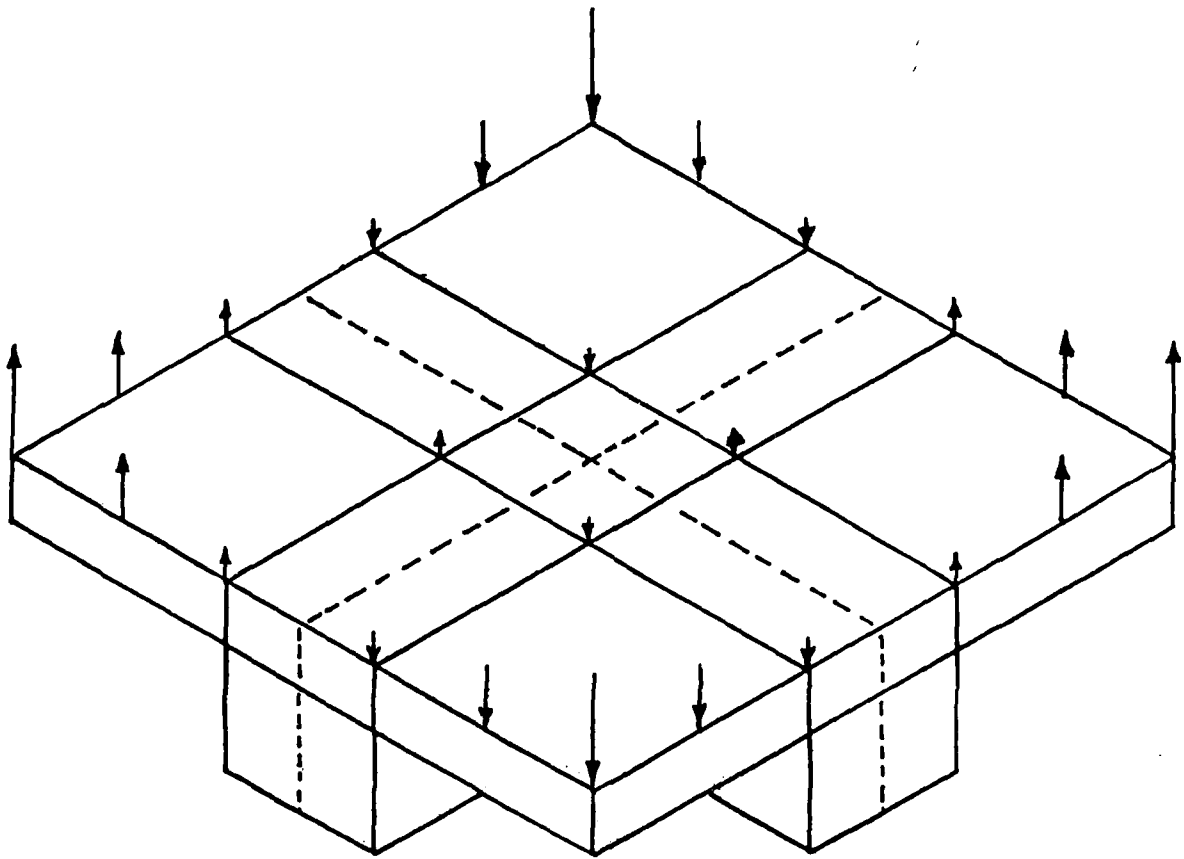
Figure 33. 1st Mode, 64.97 Hz, Iso-Pad (NASTRAN)
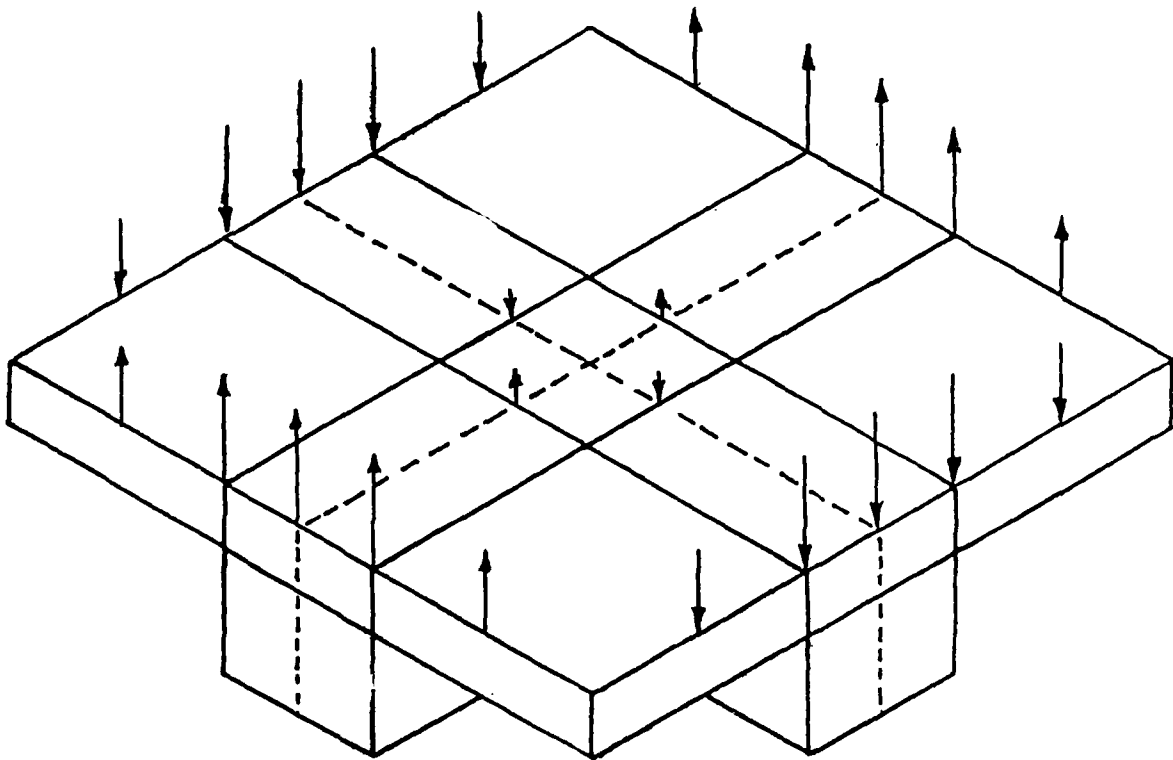
Figure 34. 2nd Mode, 81.06 Hz, Iso-Pad (NASTRAN)
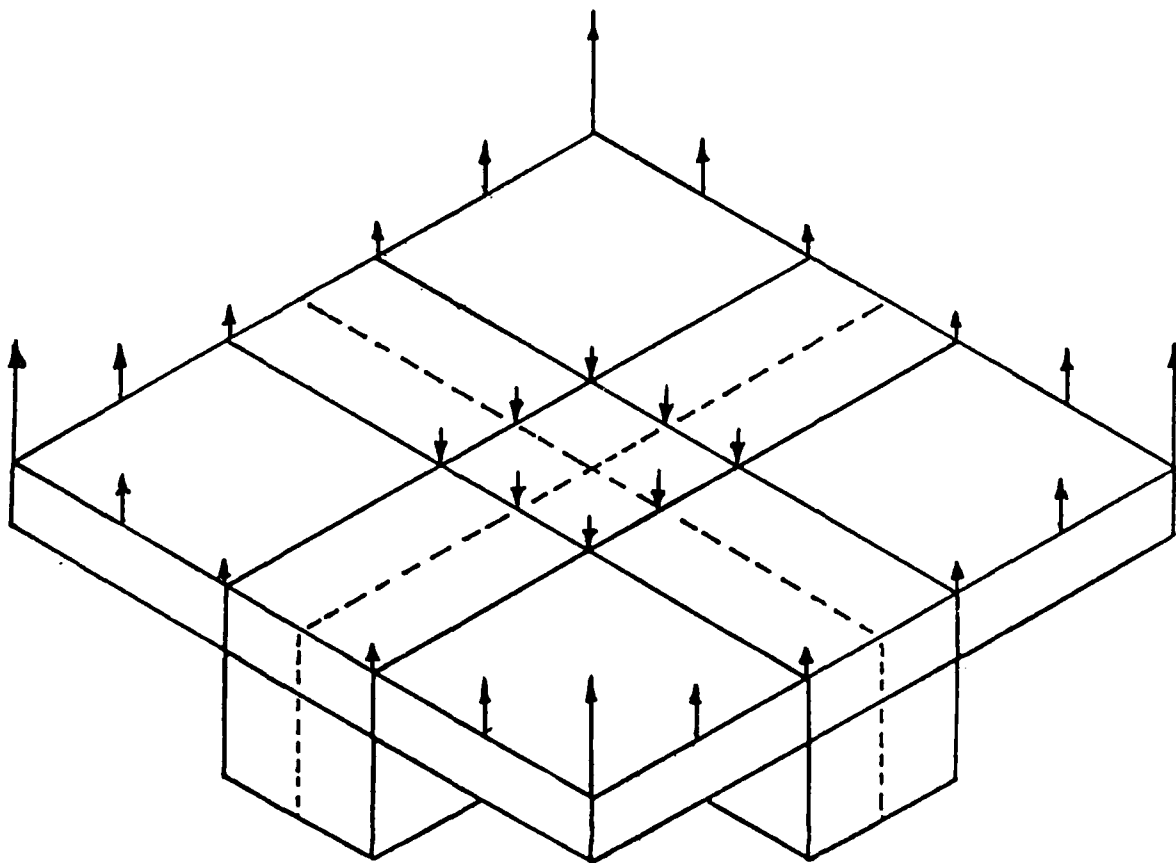
Figure 35.   3rd Mode, 86.08 Hz, Iso-Pad (NASTRAN)

53
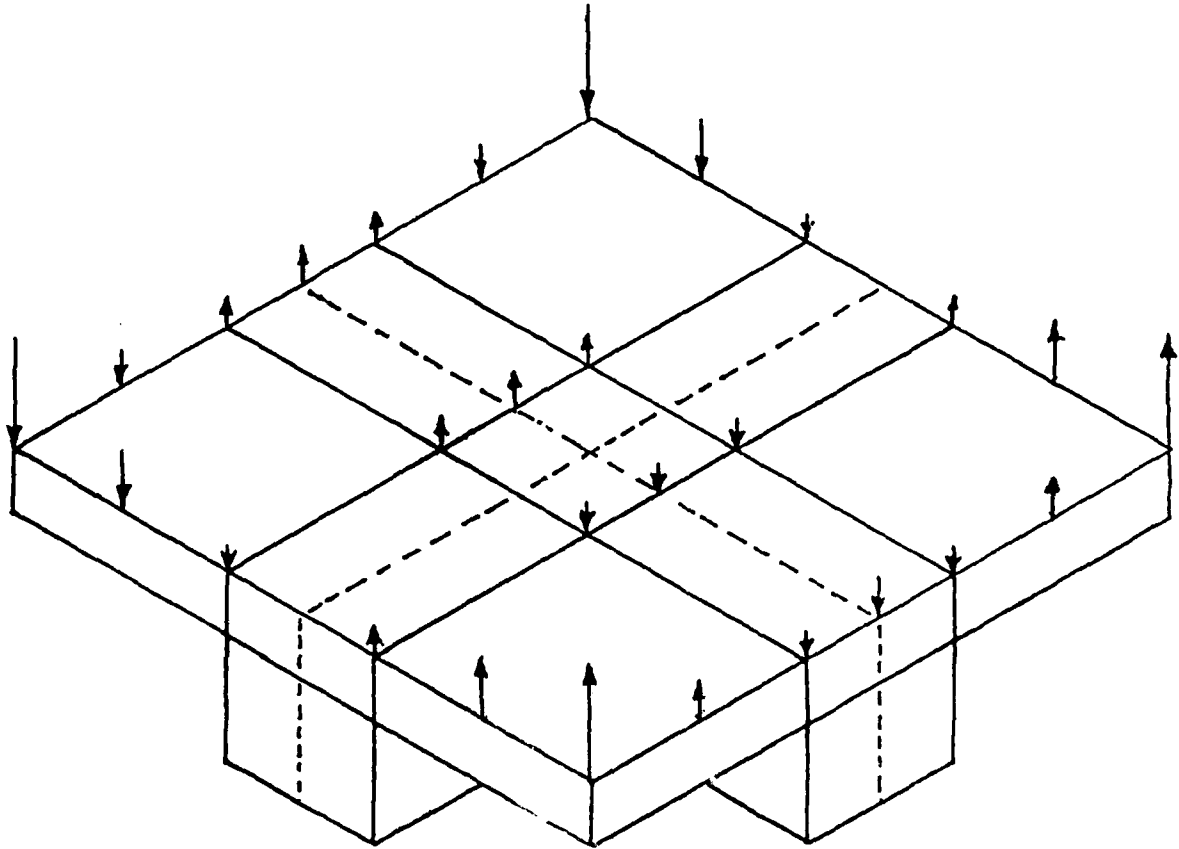
Figure 36. 4th Mode, 95.80 Hz, Iso-Pad (NASTRAN)

54
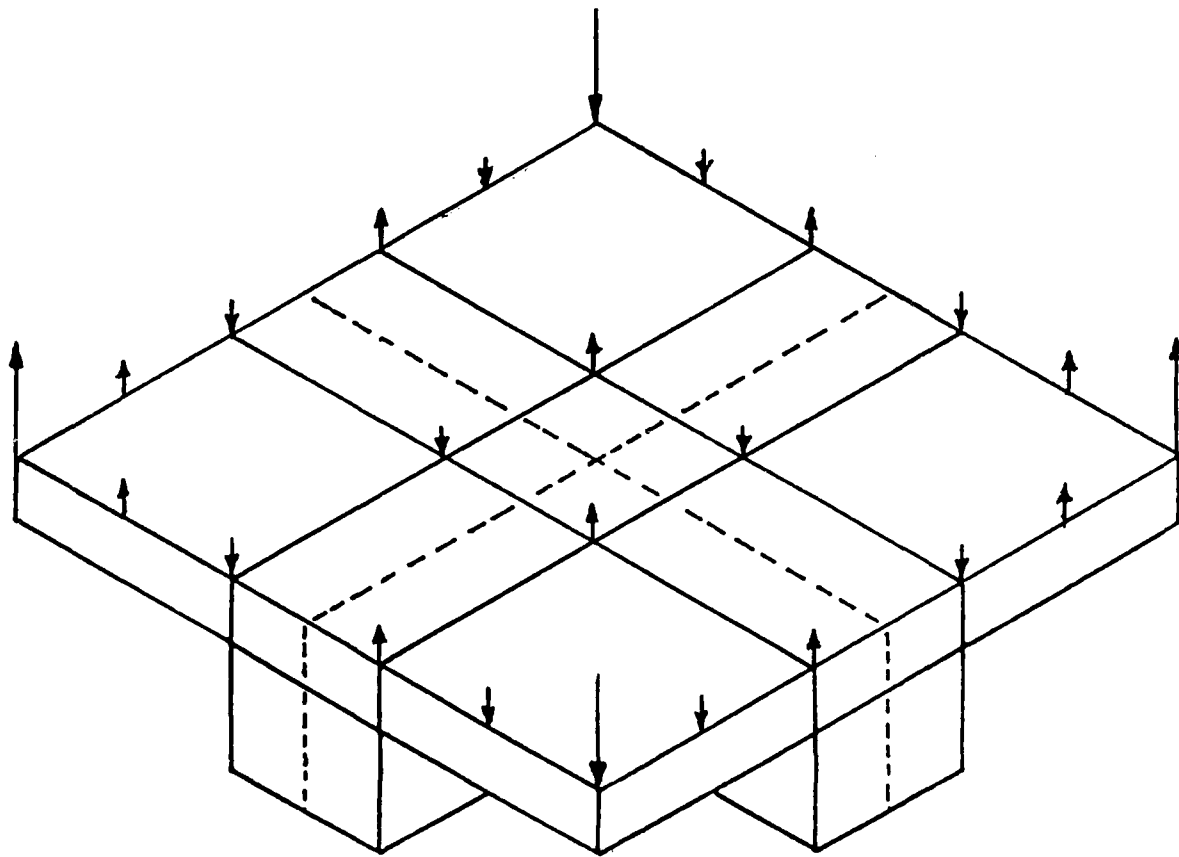
Figure 37. 5th Mode, 167.59 Hz, Iso-Pad (NASTRAN)
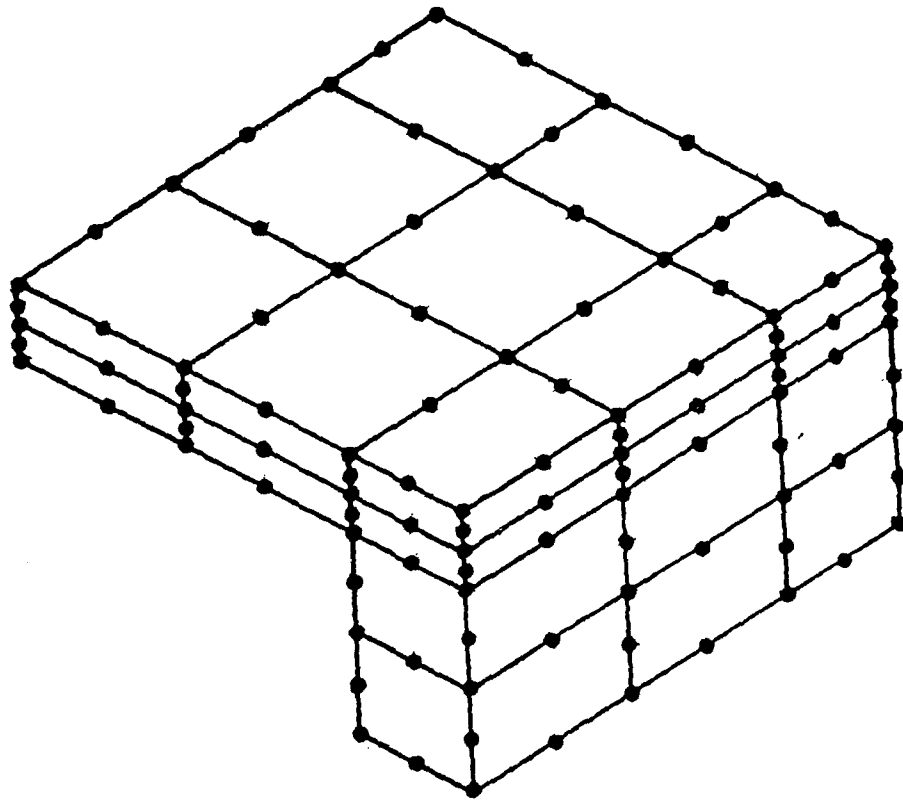
Figure 38. NASTRAN Symmetry Model, Iso-Pad
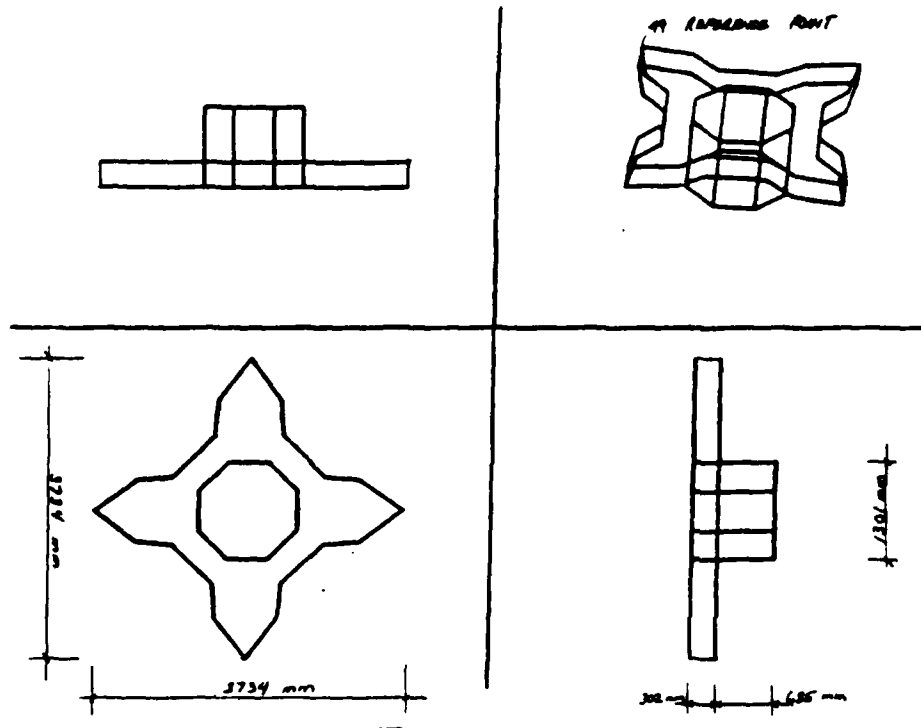
Figure 39. Orthogonal View, SSP Primary Mass
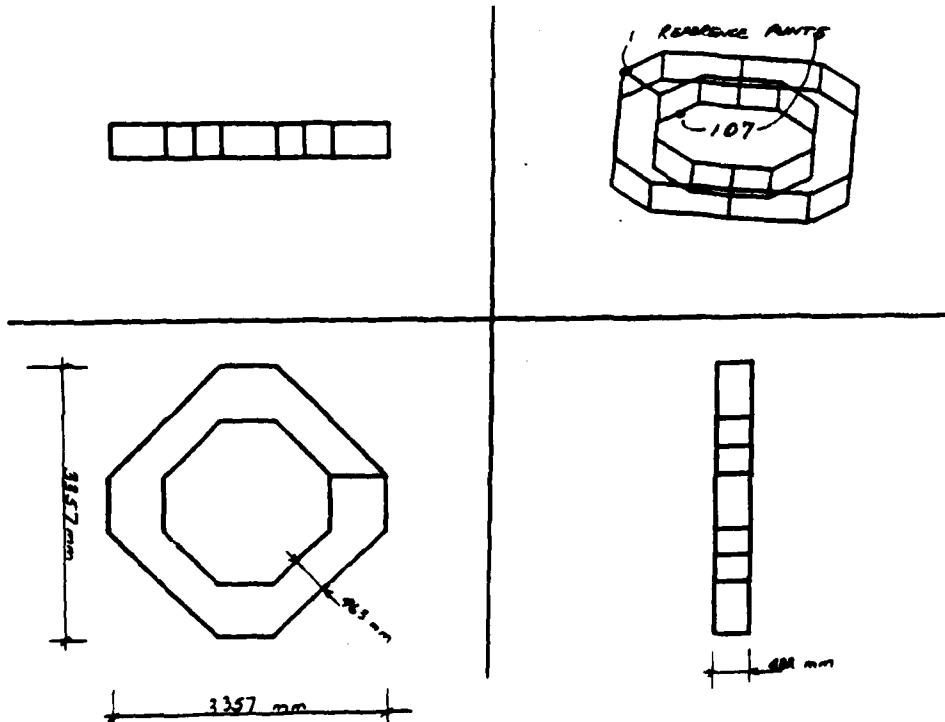
Figure 40. Orthogonal View, SSP Secondary Mass
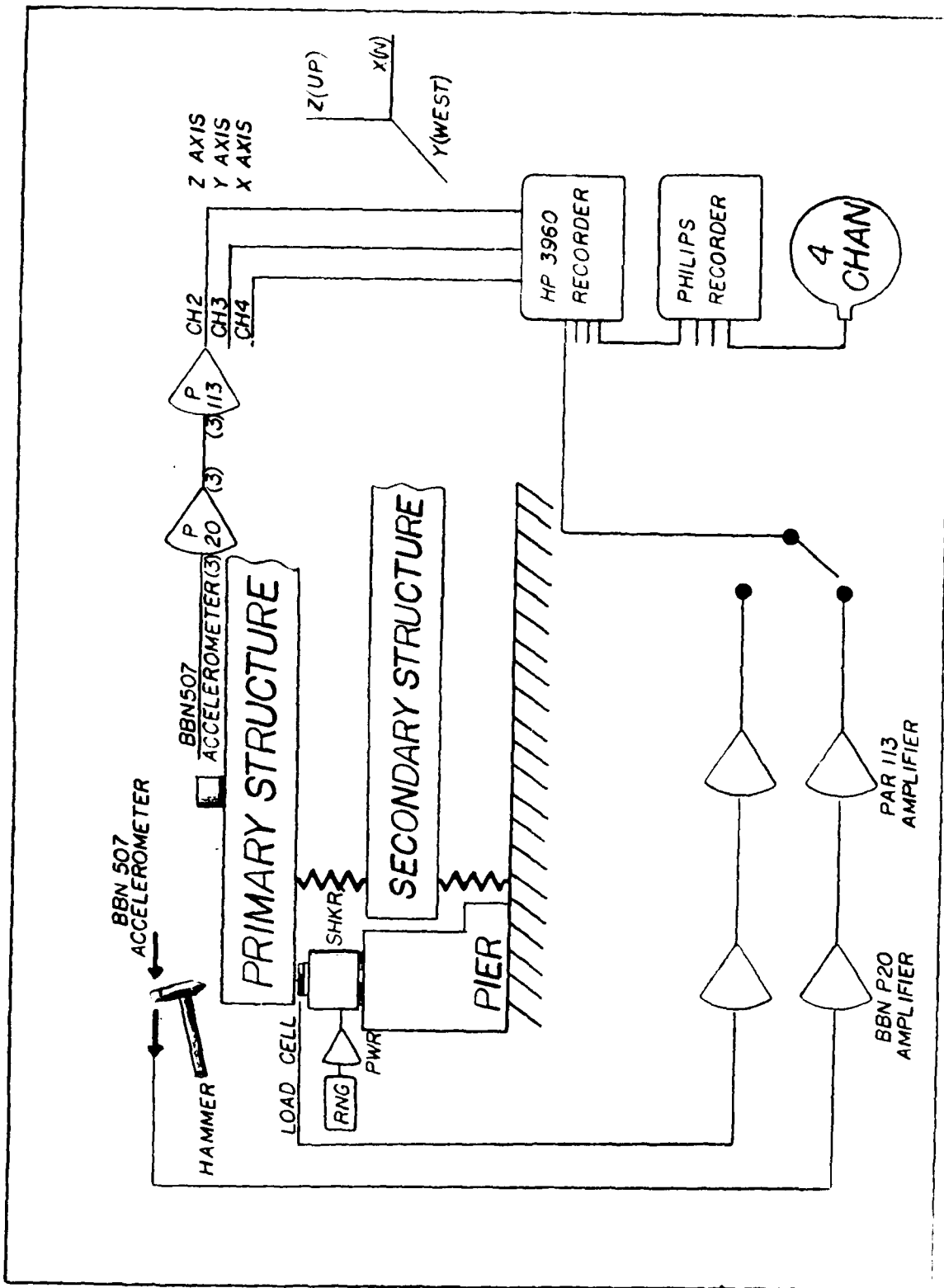
Figure 41. SSP Structural Test Set-up

58
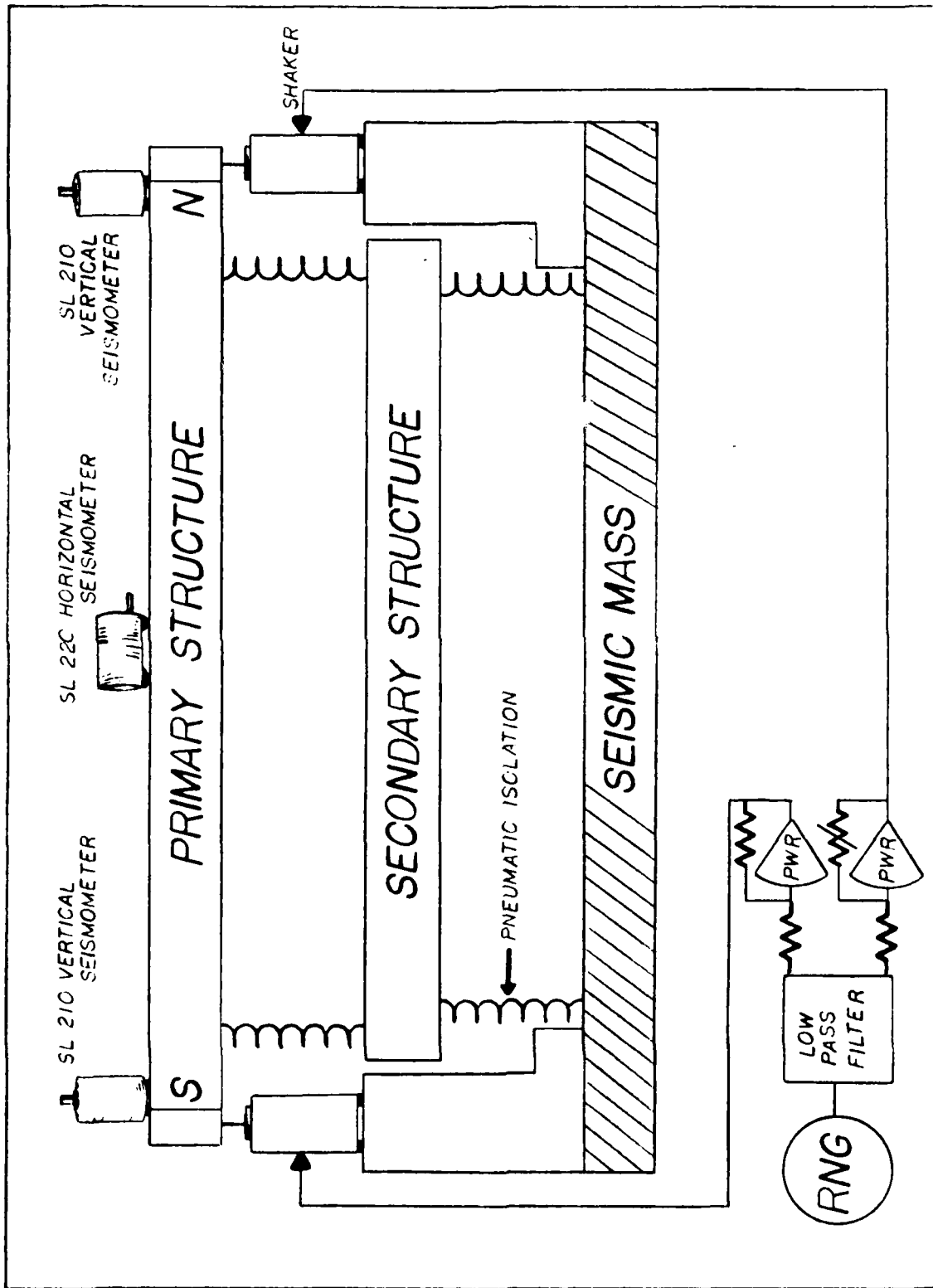
Figure 42. Test Set-up for SSP Response in the Active Control Band

(a) Oblique View

(b) Front View

Figure 44. 2nd Mode, 137 Hz, Primary Mass
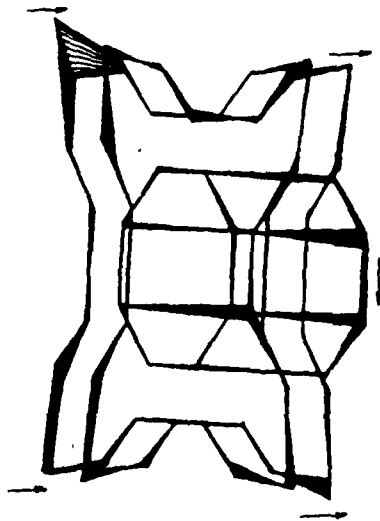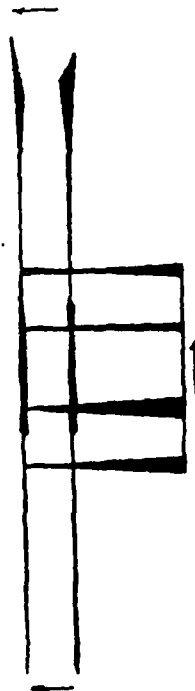
(a) Oblique View

(b) Front View

Figure 43. 1st Mode, 89 Hz, Primary Mass

60
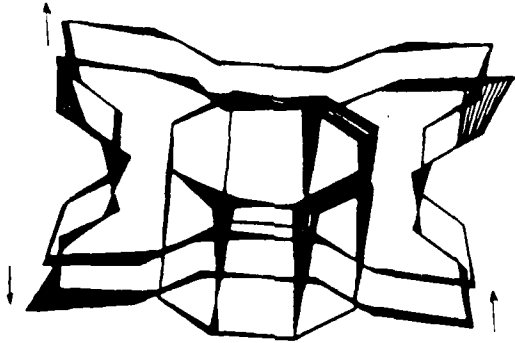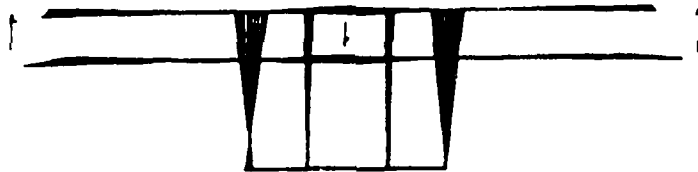
(a) Oblique View

(b) Front View

Figure 45.   3rd Mode, 335 Hz, Primary Mass

(a) Oblique View

(b) Front View
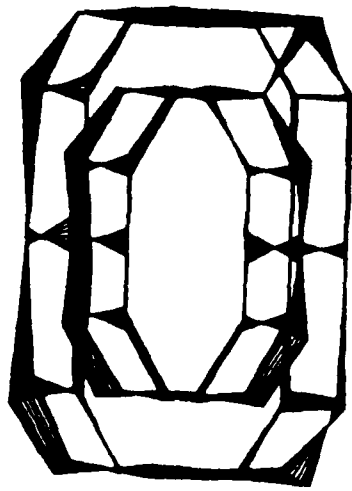
Figure 47. 2nd Mode, 150 Hz, Secondary Mass
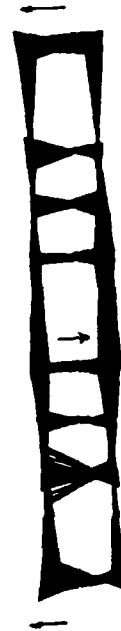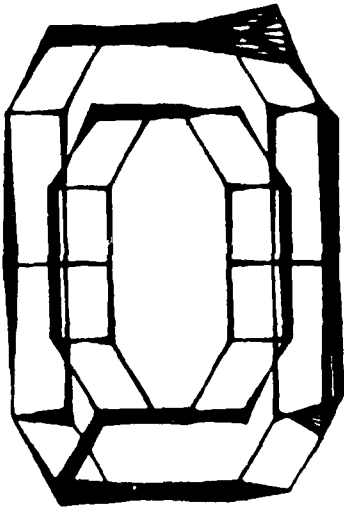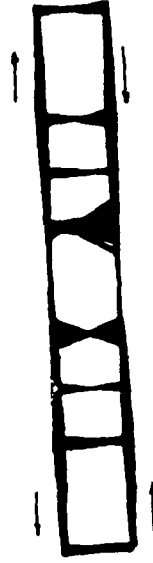
(a) Oblique View

(b) Front View

Figure 46. 1st Mode, .01 Hz, Secondary Mass

62
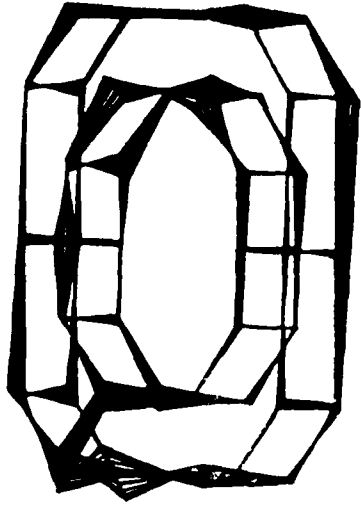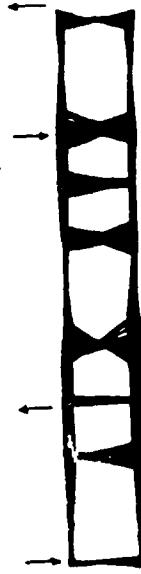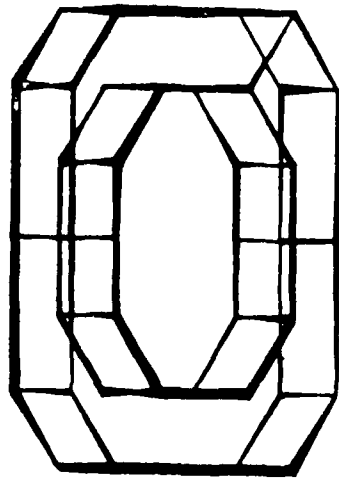
(a) Oblique View

(b) Front View

Figure 49. 4th Mode, 294 Hz, Secondary Mass

(a) Oblique View

(b) Front View

Figure 48. 3rd Mode, 279 Hz, Secondary Mass
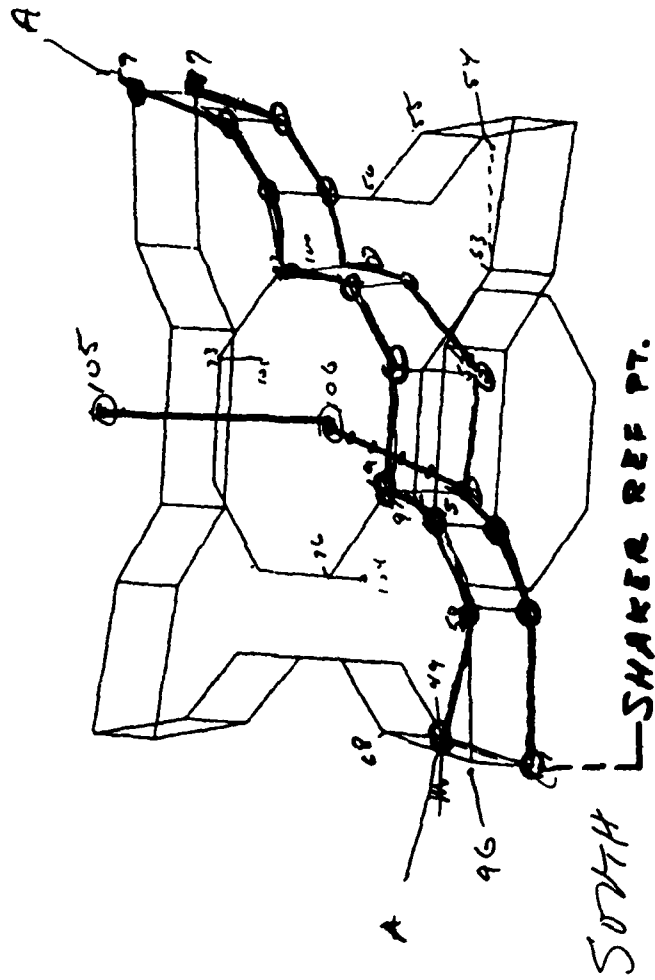
Figure 50. Primary Mass Geometry, Random Excitation
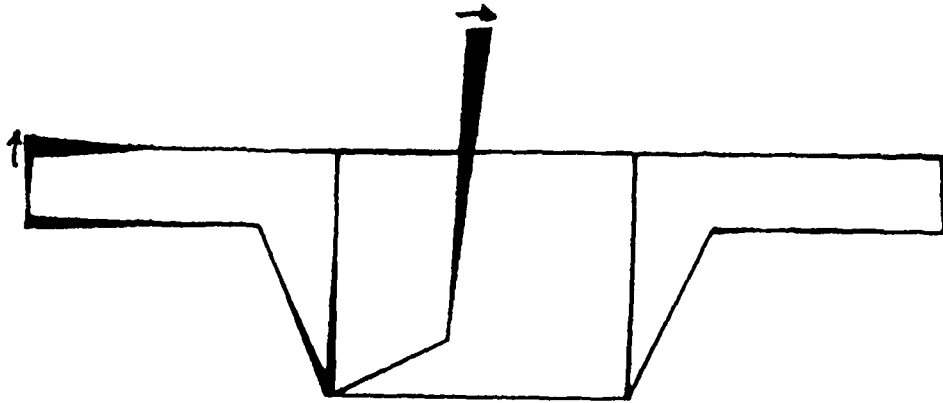
Figure 51. 40 Hz Mode, Primary Mass, Random Excitation
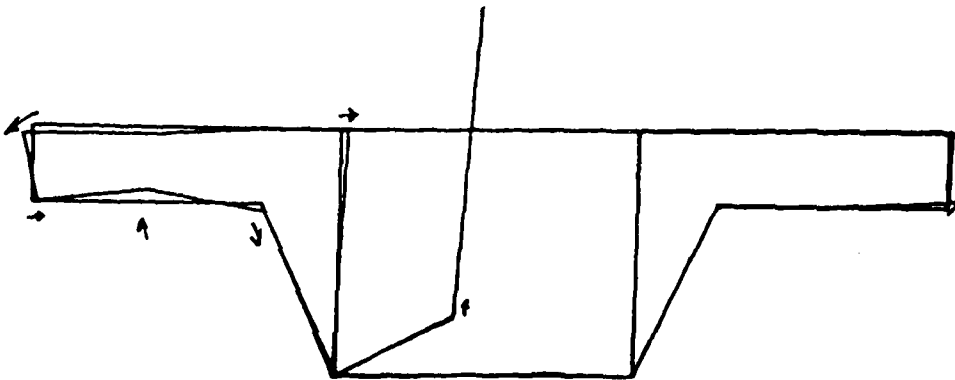

Figure 52. 61 Hz Mode, Primary Mass, Random Excitation
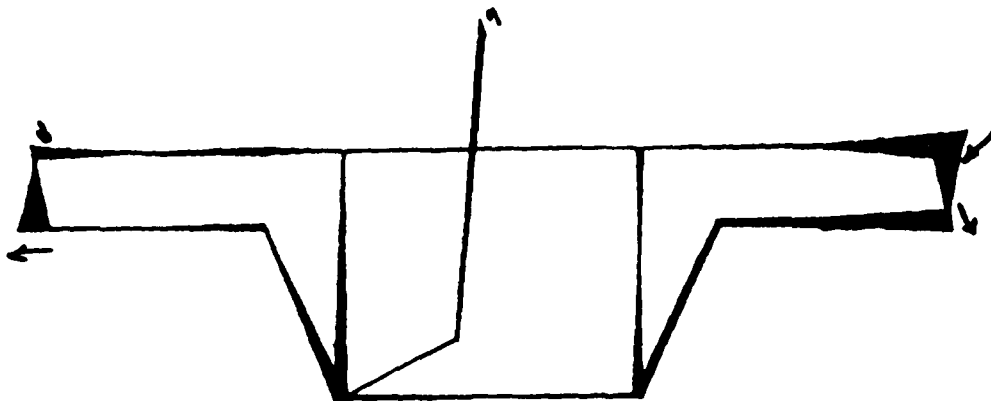
Figure 53.   87 Hz Mode, Primary Mass, Random Excitation
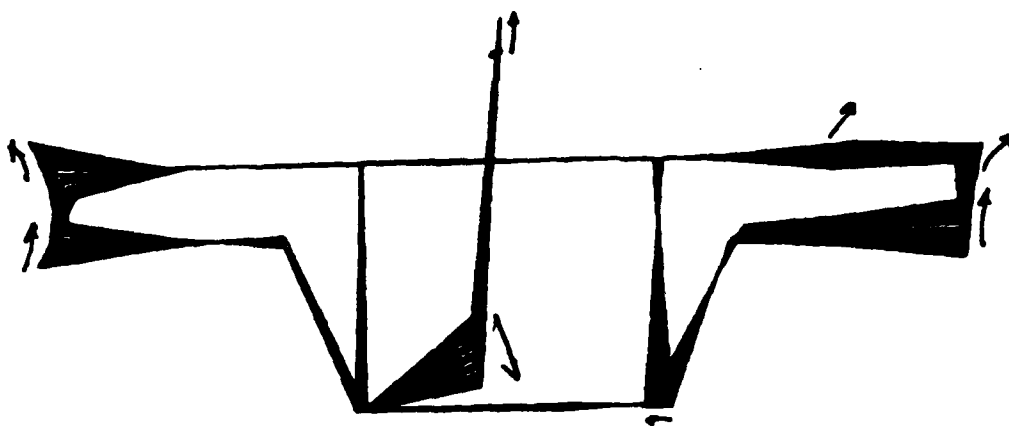
Figure 54.   95 Hz Mode, Primary Mass, Random Excitation
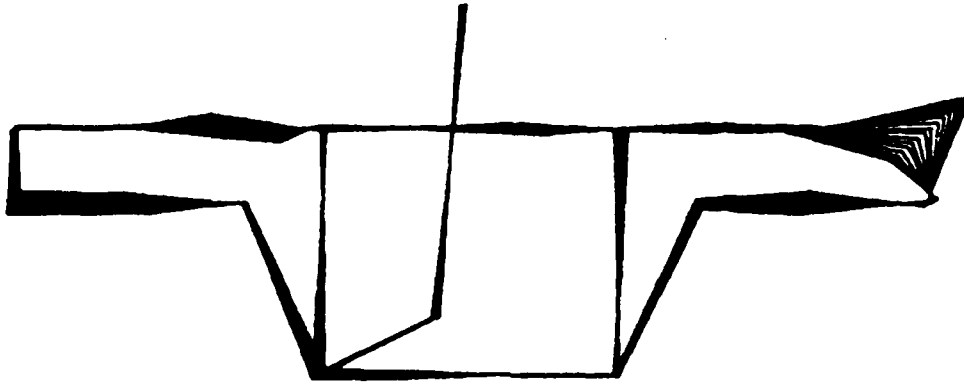
Figure 55.   120 Hz Mode, Primary Mass, Random Excitation
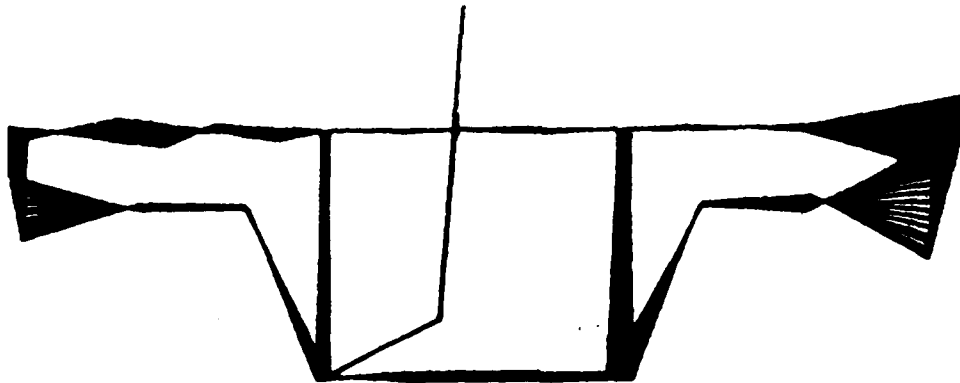


Figure 56.   142 Hz Mode, Primary Mass, Random Excitation

67
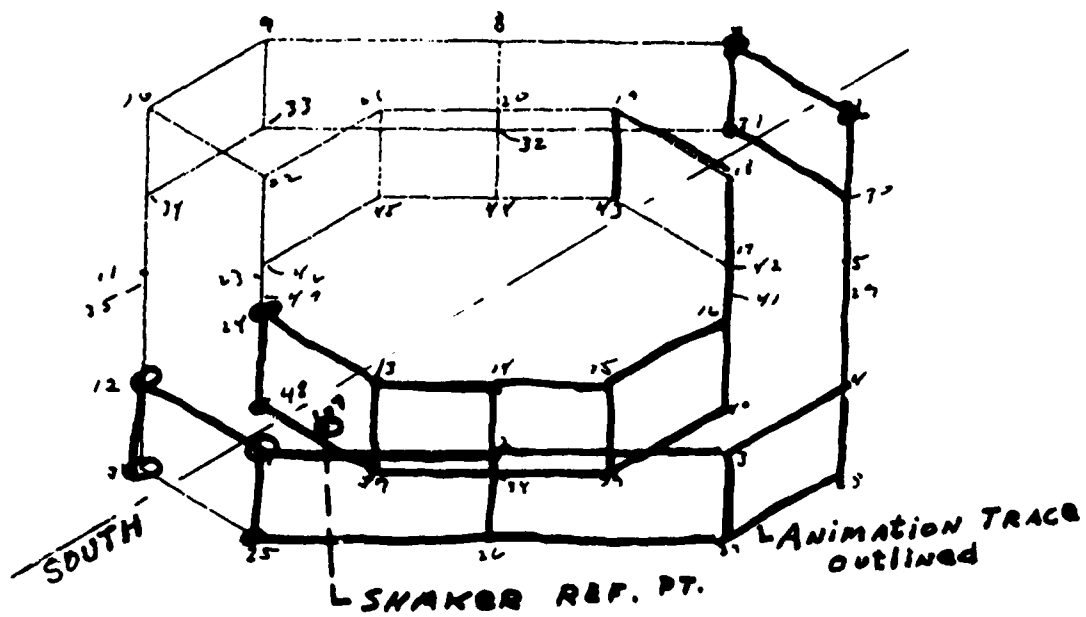
Figure 57.   Secondary Mass Geometry, Random Excitation
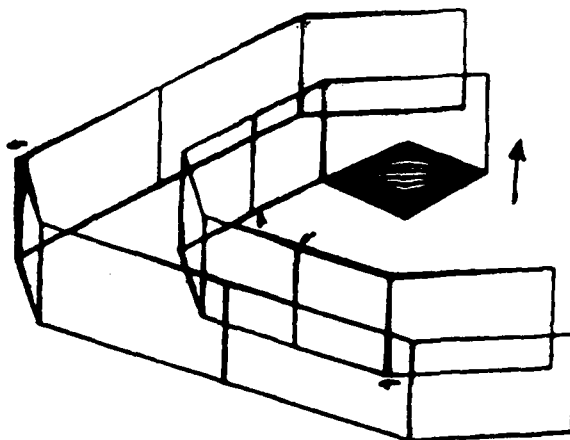
Figure 58.   22 Hz Mode, Secondary Mass, Random Excitation
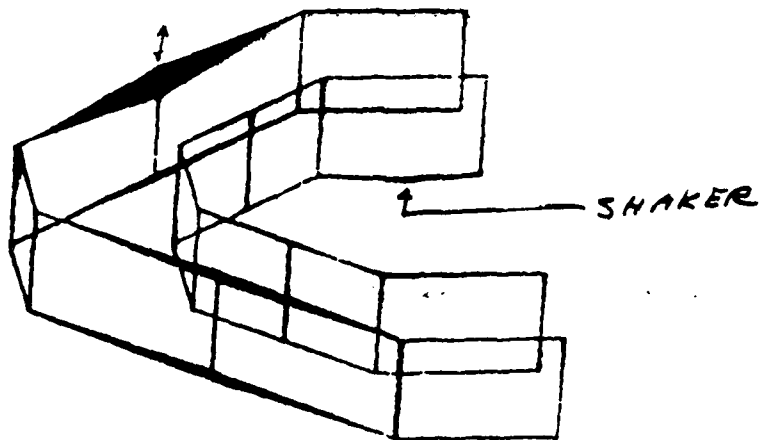
Figure 59. 50 Hz Mode, Secondary Mass, Random Excitation
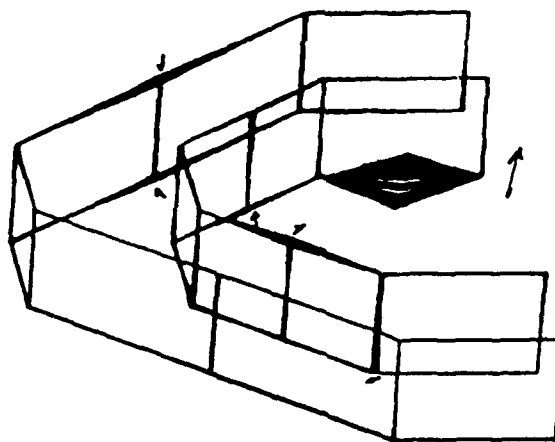
Figure 60. 62 Hz Mode, Secondary Mass, Random Excitation
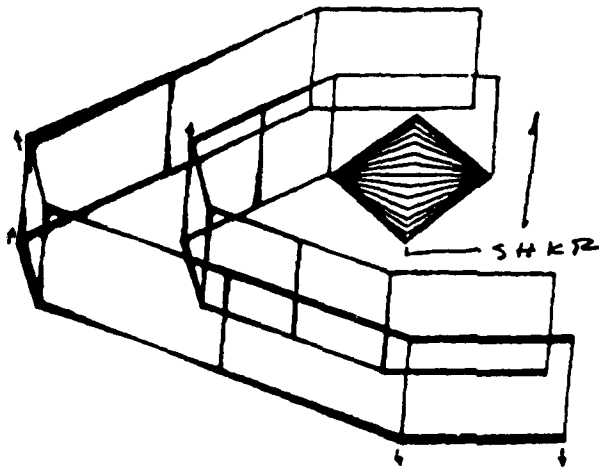
Figure 61.   90 Hz Mode, Secondary Mass, Random Excitation
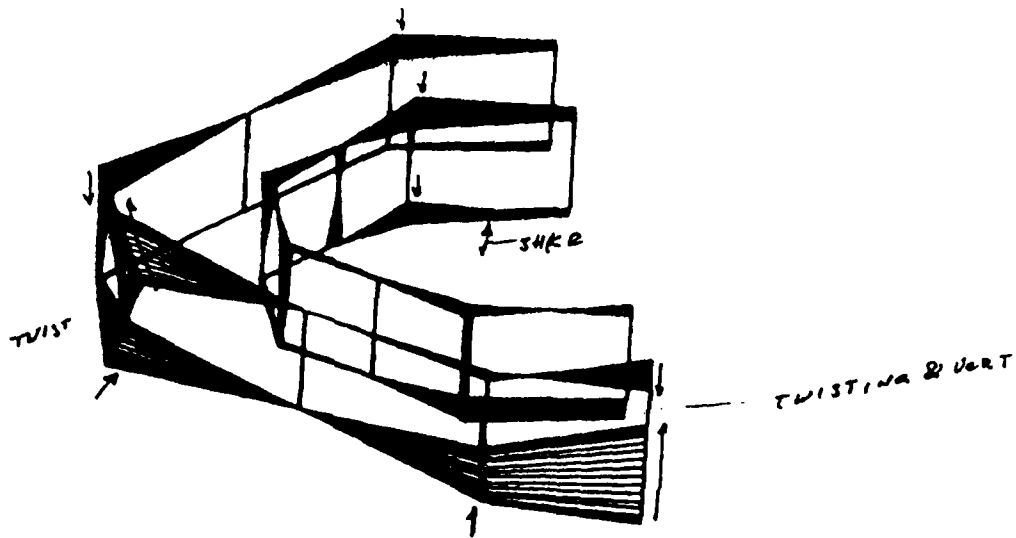
Figure 62.   101 Hz Mode, Secondary Mass, Random Excitation
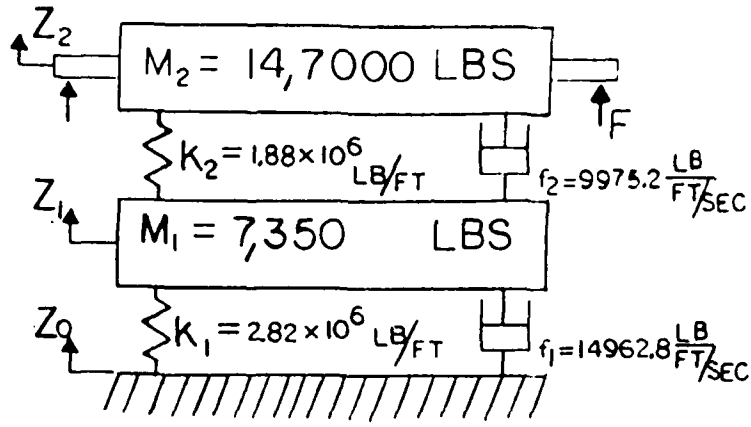
Figure 63. Dynamic Model Schematic
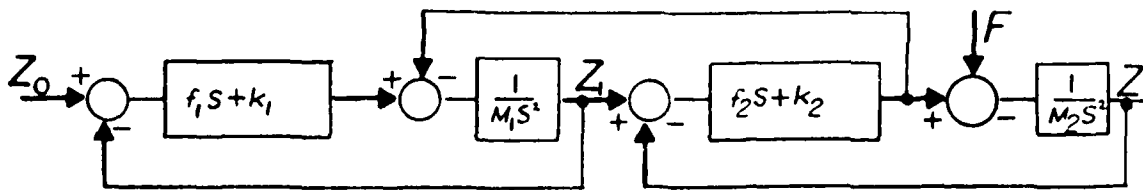
Figure 64. Vertical Translation Model

$$\frac{Z_2}{Z_0} = \frac{1\left(\frac{f}{30}+1\right)}{Q(1336,.0223)Q(4202,.07)}$$
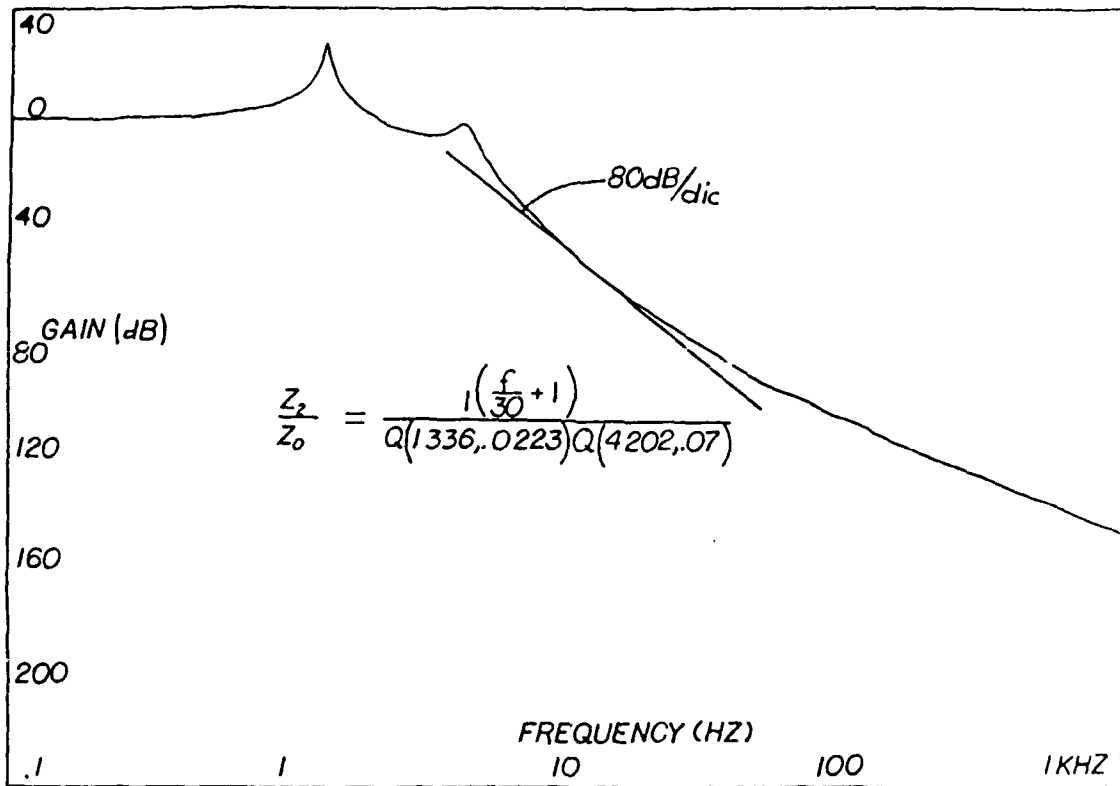
Figure 65. Theoretical Vertical Isolation

Figure 66. System Model